Motion of a rolling sphere on an azimuthally symmetric surface

D.M. Marín Quiroz
Instituto Tecnológico y de Estudios Superiores de Monterrey,
Barranca del Cobre 256, 54023, Lomas de Valle Dorado, Estado de México, México.
e-mail: danielmarin0051@gmail.com

Received 1 November 2018; accepted 28 January 2019

This paper analyzes the translational motion that a sphere rolling over an azimuthally symmetric surface, under the presence of a constant gravitational field and with the rolling-without-slipping condition, exhibits in two different situations: with and without friction with air, where the latter is expressed as a power-series function of the sphere's translational speed. In order to achieve this, the equations of motion for each case are obtained through the use of Lagrangian Mechanics and are subsequently solved by numerical computation in *Wolfram Mathematica*. For the frictionless case, periodic behavior and a conservation law for the angular coordinate have been found, along with the condition under which an effective potential energy can be approximated as well as the relationships between initial conditions that produce gravitational-like trajectories for the motion of the sphere. The equations of motion derived for the case with friction are found to predict the energy loss and general decay of the sphere's motion. Likewise, the normal force over the sphere as a function of time is obtained through the method of *Lagrange's Undetermined Multipliers*, and thus, the general conditions that the motion must satisfy in order to be described by the obtained models. Overall, this research provides insight into the type and characteristics of the motion performed by the system in these two cases, both through equations and their numerical solutions for different surfaces and initial conditions.

Keywords: Rolling sphere; rotationally symmetric surfaces; Lagrangian Mechanics; aerodynamic friction; elliptic trajectories.

PACS: 45.20.Jj; 45.40.-f; 45.50.-j.

DOI: https://doi.org/10.31349/RevMexFisE.65.128

1. Introduction and theoretical background

Newton's formulation of Classical Mechanics often leads to a laborious endeavor when trying to identify the forces acting on and sometimes within a system in order to obtain the equations that describe its motion as a function of time. Fortunately, the Lagrangian formulation of Classical Mechanics stands out as a powerful tool to solve the motion of this kind of systems as its approach is fundamentally different from the Newtonian. In Lagrangian Mechanics, the Lagrangian $\mathcal{L}$ is the central quantity to be found through the incorporation of both the kinetic and potential energies of the system and the constraints to the motion of the bodies or particles that conform it.

Formally, the *Lagrangian* of a particle in generalized coordinates q_i is a function of these coordinates and their time derivatives; and its equal to the difference between its kinetic energy T and its potential energy V [1]

$$\mathcal{L}(q_1, \ldots, q_N, \dot{q}_1, \ldots \dot{q}_N) = T - V. \tag{1}$$

The equations of motion corresponding to each coordinate can be subsequently obtained by substituting the *Lagrangian* into the *Euler-Lagrange* equation, which for the i-th coordinate of a given coordinate system is [2]

$$\frac{d}{dt}\left(\frac{\partial \mathcal{L}}{\partial \dot{q}_i}\right) - \frac{\partial \mathcal{L}}{\partial q_i} = 0. \tag{2}$$

The main goal of the present research is to describe and predict the translational motion that a spherical rigid object would exhibit in the presence of a constant gravitational field, both with and without friction with air, over the surface of another rigid object whose shape is described by the real part of the surface Eq. (3). Figure 1 shows two possible examples of such surface.

$$z = a(\rho - h)^n \tag{3}$$

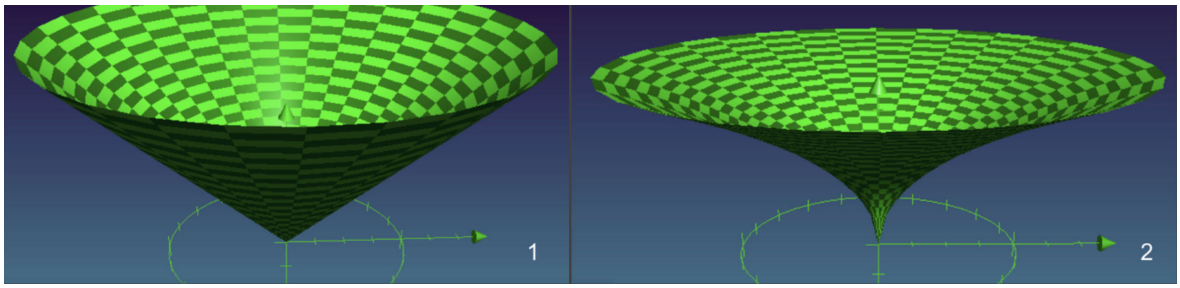

FIGURE 1. Two examples of the type of surfaces described by Eq. (3). Surface 1 (a cone) has $a = 1$, $h = 0$ and $n = 1$; Surface 2 has $a = 1$, $h = 0$ and $n = 0.5$. The z-axis points vertically up through the symmetry axis of both surfaces.

Equation (3) is stated in cylindrical coordinates, which simply are another set of coordinates axes that describe the position of any point in space by specifying the values of three cylindrical coordinates: ρ, ϕ, and z, which are commonly called the *radius*, *azimuth*, and *height* coordinates, respectively. Their mathematical connection with the cartesian coordinate system is stated in the following set of equations, including their unit vectors and the equation for velocity in this particular coordinate system [3]:

$$\begin{aligned} x &= \rho\cos\phi \quad y = \rho\sin\phi \quad z = z \\ \hat{\rho} &= \hat{x}\cos\phi + \hat{y}\sin\phi \\ \hat{\phi} &= -\hat{x}\sin\phi + \hat{y}\cos\phi \quad z = z \\ \vec{v} &= \dot{\rho}\hat{\rho} + \rho\dot{\phi}\hat{\phi} + \dot{z}\hat{z}. \end{aligned} \tag{4}$$

Figure 2 shows the diagram of a standard cylindrical coordinate system with its corresponding unit vectors. For this kind of coordinate system we have that the generalized coordinates q_i take the following form:

$$\begin{aligned} q_1 &= \rho \quad \dot{q}_1 = \dot{\rho} \\ q_2 &= \phi \quad \dot{q}_2 = \dot{\phi} \\ q_3 &= z \quad \dot{q}_3 = \dot{z}. \end{aligned}$$

The family of surfaces in which this investigation is concerned about has the characteristic of being rotationally symmetric around the z-axis, or in other words, it exhibits *azimuthal* symmetry, which is implicitly present in Eq. (3) by the independence of the z-coordinate on the ϕ-coordinate.

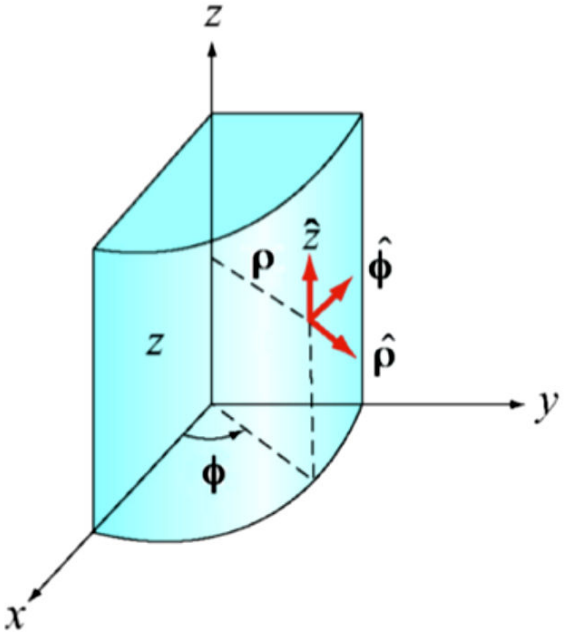

FIGURE 2. Diagram of a standard cylindrical coordinate system with radius ρ, azimuth ϕ, and height z (MIT, 2005, p. 6).

For the sake of simplicity it is also considered that the constant gravitational field points along the negative z-axis, and thus interacts with any object in the form of gravitational potential energy described by

$$V(z) = mgz. \tag{5}$$

Throughout this research, the obtained solutions are analyzed for arbitrarily selected special cases with the *Wolfram Mathematica* software to illustrate the behavior of the system in two and three dimensions, as well as the motion in each coordinate as a function of time. In order to achieve this, the results are presented in the form of plots and graphs which represent the solutions to the equations of motion obtained by giving the software enough parameters to calculate. These parameters will be specified for each case.

It is worth mentioning that, as a consequence of the solution's generality, the measurement system used in this research may well be any self-consistent and well-defined measurement system, but in order to stick with international standards, all the quantities presented on this research are given in the International System of Units. For example, if z and ρ from the surface Eq. (3) are quantities that represent distance and thus have units of length, and taking into consideration that the exponent n is a unitless constant, then both z and ρ are measured in meters m and the constants h and a are given in m and m^{1-n} respectively, letting us preserve the consistency of our units.

2. Frictionless model

2.1. Derivation of the equations of motion

Let us derive the equations of motion for a solid sphere rolling on top of any surface described by Eq. (3), under the assumptions that the rolling-without-slipping condition (see Eq. (8)) is met for every time t and that there is no energy loss caused by dissipative forces like friction (whether with air or with the surface itself). Let us also approximate the motion in such a way that we are able to assume that the object's center of mass lies in the point of contact with the surface, which could actually be done if we demand the condition that the radius r of the sphere is sufficiently small such that the fixed normal distance r of the sphere's center of mass to the point of contact with the surface is negligible.

By computing the scalar product of Eq. (4) for the sphere's velocity with itself, we find the equation for the we find that the equation for the squared speed is:

$$|\vec{v}|^2 = \dot{\rho}^2 + \rho^2\dot{\phi}^2 + \dot{z}^2. \tag{6}$$

Let us consider a solid sphere whose moment of inertia around an axis parallel to the immediate surface on which the object lies (and therefore around the axis on which it momentarily rotates) is described by the following equation

$$I = kmr^2, \tag{7}$$

where k is a dimensionless constant that may take any value from cero (if the mass is concentrated almost entirely on the sphere's center) to 2/3 (the corresponding value of k for a hollow sphere). As an example we could have $k = 2/5$ for a uniformly solid sphere.

With this in mind, let us recall that the rolling-without-slipping condition takes the following form

$$|\vec{\omega}| = \frac{|\vec{v}|}{r}, \tag{8}$$

where $\vec{\omega}$ is the angular velocity vector that describes the sphere's rotation around its rotational axis. By using Eqs. (6), (7) and (8), we are able to write the equation for the total kinetic energy T of the sphere

$$\begin{aligned} T &= \frac{1}{2}m|\vec{v}|^2 + \frac{1}{2}I|\vec{\omega}|^2 = \frac{1}{2}m|\vec{v}|^2 + \frac{1}{2}mk|\vec{v}|^2 \\ &= \frac{1}{2}m(1+k)|\vec{v}|^2. \end{aligned} \tag{9}$$

In addition, it can be observed that the surfaces described by Eq. (3) represent an holonomic constraint to the motion of our object. An holonomic constraint is simply a constraint that can be written as a relationship between the coordinates being used and does not depend on the path that our object has taken. This constraint can be used to reduce the number of coordinates on which the *Lagrangian* depends.

In order to achieve this, let us find the squared time derivative of Eq. (3) which, as a consequence of its role as constraint of the sphere's motion, also represents the height z of the sphere for every time t (the limits for this condition are explored in the section *Limitations of the Model*):

$$\dot{z}^2 = a^2n^2(\rho - h)^{2(n-1)}\dot{\rho}^2. \tag{10}$$

By substituting the Eq. (10) and the surface Eq. (3) into (6) and (5), respectively, we are able to find the equations for the squared speed and potential energy solely as functions of ρ, $\dot{\rho}$ and $\dot{\phi}$:

$$|\vec{v}|^2 = (1 + a^2n^2(\rho - h)^{2(n-1)})\dot{\rho} + \rho^2\dot{\phi}^2 \tag{11}$$

$$V(\rho) = amg(\rho - h)^n. \tag{12}$$

Likewise, by substituting the kinetic energy Eq. (9) into the Lagrangian (1) we get:

$$\mathcal{L}(q_1, \ldots, q_N, \dot{q}_1, \ldots \dot{q}_N) = \frac{1}{2}m(1+k)|\vec{v}|^2 - V.$$

or, with Eqs. (11) and (12):

$$\begin{aligned} \mathcal{L}(\rho, \dot{\rho}, \dot{\phi}) = \frac{1}{2}m(1+k) \\ \times ((1 + a^2n^2(\rho - h)^{2(n-1)})\dot{\rho}^2 + \rho^2\dot{\phi}^2) \\ - amg(\rho - h)^n. \end{aligned} \tag{13}$$

For q_1 and q_2 we have the following results for the corresponding partial derivatives:

$$\begin{aligned} \frac{\partial \mathcal{L}}{\partial \rho} &= m(1+k)\Big[a^2n^2(n-1)(\rho-h)^{2n-3}\dot{\rho}^2 \\ &\quad + \rho\dot{\phi}^2 - \frac{ang(\rho-h)^{n-1}}{(1+k)}\Big] \\ \frac{\partial \mathcal{L}}{\partial \dot{\rho}} &= m(1+k)(1 + a^2n^2(\rho-h)^{2(n-1)})\dot{\rho} \\ \frac{d}{dt}\left(\frac{\partial \mathcal{L}}{\partial \dot{\rho}}\right) &= m(1+k)\Big[(1 + a^2n^2(\rho-h)^{2(n-1)})\ddot{\rho} \\ &\quad + 2a^2n^2(n-1)(\rho-h)^{2n-3}\dot{\rho}^2\Big] \\ \frac{\partial \mathcal{L}}{\partial \phi} &= 0 \\ \frac{\partial \mathcal{L}}{\partial \dot{\phi}} &= m(1+k)\rho^2\dot{\phi} \\ \frac{d}{dt}\left(\frac{\partial \mathcal{L}}{\partial \dot{\phi}}\right) &= m(1+k)[\rho^2\ddot{\phi} + 2\rho\dot{\rho}\dot{\phi}]. \end{aligned} \tag{14}$$

Therefore, the Euler-Lagrange equation (1) takes the following form for each coordinate:

$$\frac{d}{dt}\left(\frac{\partial \mathcal{L}}{\partial \dot{\rho}}\right) - \frac{\partial \mathcal{L}}{\partial \rho} = 0 \tag{15}$$

$$\frac{d}{dt}\left(\frac{\partial \mathcal{L}}{\partial \dot{\phi}}\right) = 0 \leftrightarrow \frac{\partial \mathcal{L}}{\partial \dot{\phi}} = \text{constant}, \tag{16}$$

where from (16) we have now found that ϕ is an ignorable coordinate, which is a direct consequence of the system's azimuthal symmetry. By substituting the derivatives from (14) into Eqs. (15) and (16) we obtain the following two equations of motion:

$$\begin{aligned} m(1+k)\Big[(1 + a^2n^2(\rho-h)^{2(n-1)})\ddot{\rho} + a^2n^2(n-1) \\ \times (\rho-h)^{2n-3}\dot{\rho}^2 - \rho\dot{\phi}^2 - \rho\dot{\phi}^2 \\ + \frac{ang(\rho-h)^{n-1}}{(1+k)}\Big] = 0 \end{aligned} \tag{17}$$

$$m(1+k)\rho^2\dot{\phi} \equiv (1+k)L_z. \tag{18}$$

In the last step the constant $(1+k)L_z$ has been introduced, where $L_z = m\rho^2\dot{\phi}$ represents the z-component of the angular momentum of the object's center of mass with respect to the origin, a quantity that must be conserved according to Eq. 16, and thus, lets us already derive its own conservation law. Because this quantity keeps constant along the complete motion of the sphere, its magnitude must always be the same regardless of time, including at $t = 0$ (which can be arbitrarily selected), where we have:

$$L_z = m\rho(0)^2\dot{\phi}(0) = \text{constant}. \tag{19}$$

By substituting this last equation into the equation of motion for the ϕ coordinate (18) we get:

$$\dot{\phi} = \frac{\rho(0)^2\dot{\phi}(0)}{\rho^2}. \tag{20}$$

Likewise, by substituting Eq. (20) into Eq. (17) and dividing by m and $(1+k)$ - which we assume not to be equal to cero - we finally get a nonlinear ordinary differential equation for ρ (see Eq. (21)), whose solution lets us immediately know the motion of the sphere along the ϕ and z coordinates, the former by direct integration of Eq. (20), and the latter by direct substitution into the surface Eq. (3), letting the sphere's translational motion be fully described by the following set of equations:

$$\begin{aligned}&(1 + a^2n^2(\rho - h)^{2(n-1)})\ddot{\rho} + a^2n^2(n-1)\\ &\times (\rho - h)^{2n-3}\dot{\rho}^2 - \frac{\rho(0)^4\dot{\phi}(0)^2}{\rho^3}\\ &+ \frac{ang(\rho - h)^{n-1}}{(1+k)} = 0\end{aligned} \tag{21}$$

$$\phi(t) = \int \frac{\rho(0)^2\dot{\phi}(0)}{\rho(t)^2}dt \tag{22}$$

$$z = a(\rho - h)^n. \tag{23}$$

These equations can be numerically solved when all of the following parameters are specified:

- Three surface constants: a, h, n
- One rigid body parameter: k
- One gravitational constant: g
- Four initial conditions: $\rho(0)$, $\dot{\rho}(0)$, $\phi(0)$, and $\dot{\phi}(0)$.

2.2. Analysis of special cases without friction

In order to show the solutions to the motion described by Eqs. 21, 22, and 23, we proceed to analyze their predictions for certain special cases. Surfaces one through six (-shown in Fig. 3, along with the geometrical parameters and initial

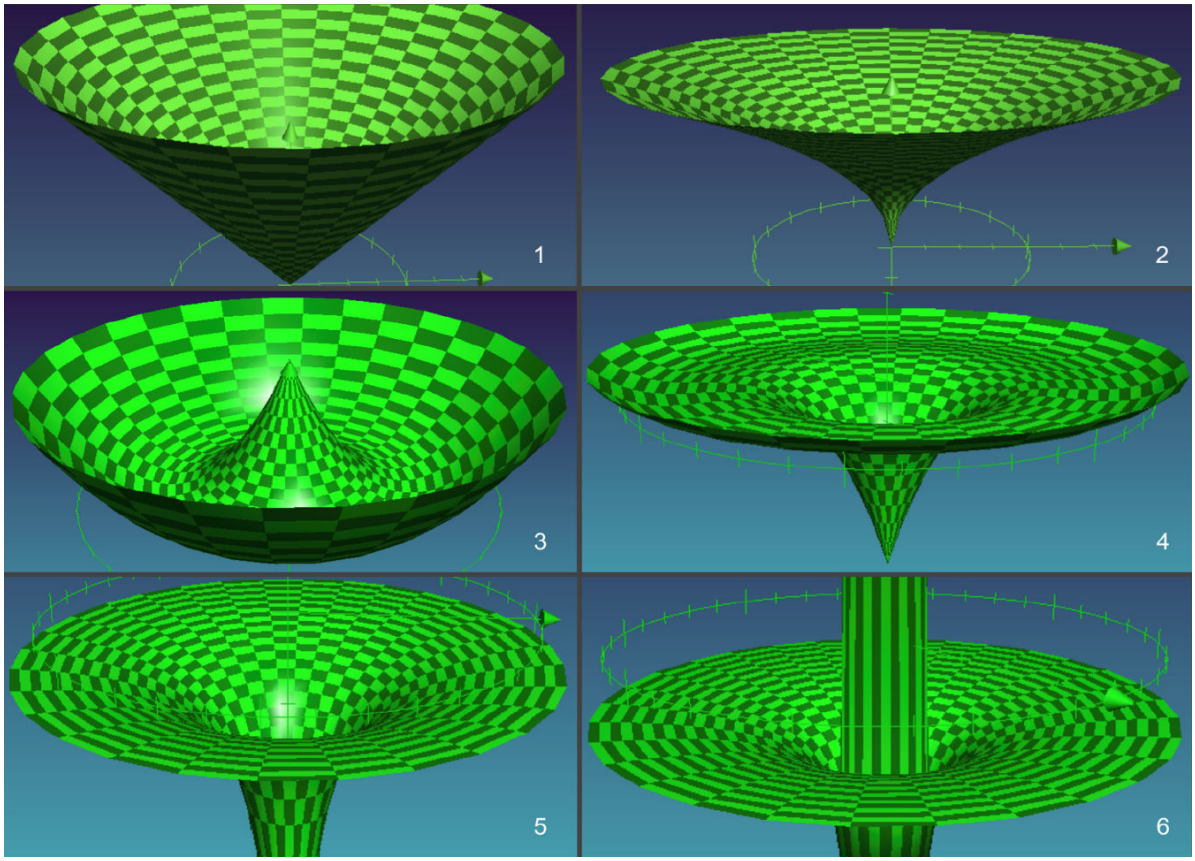

FIGURE 3. Six special cases to analyze. Surfaces 1, 2, 3, 4, 5, and 6 are described by Eq. (3) and correspond to the following a, h, and n values: Surface 1: (1, 0, 1), Surface 2: (1, 0, 0.5), Surface 3: (1, 2, 2), Surface 4: (0.2, 1.8, 3), Surface 5: (-1, 0, -1), and Surface 6: (-0.1, 0.08, -1/3). Surface 6 shows a central protuberance due to the existence of a vertical asymptote in $\rho = h = 0.08$. Such protuberance in the region $-h < \rho < h$ is not correctly depicted by the computer software used. The reader can safely ignore such region since it never interacts with the motion of the sphere as long as the sphere's radius remains negligible, its motion satisfies $\rho(0) > h$, and it always keeps in contact with the surface.

values indicated) have been selected to be analyzed as these special cases to illustrate the behavior of the system. The following are the sets of corresponding parameters

$$\left\{\{a_j, h_j, n_j\}, \{k_j\}, \{g_j\}, \{\rho(0)_j, \dot{\rho}(0)_j, \phi(0)_j, \dot{\phi}(0)_j\}\right\}$$

being corresponded by (recalling that k and n are dimensionless) the units set

$$\left\{\{\mathrm{m}^{1-n}, \mathrm{m}, (\text{no units})\}, \{(\text{no units})\}, \left\{\frac{\mathrm{m}}{\mathrm{s}^2}\right\}, \left\{\mathrm{m}, \frac{\mathrm{m}}{s}, \mathrm{rad}, \frac{\mathrm{rad}}{\mathrm{s}}\right\}\right\}$$

for each j-th special case to be analyzed, with $j = 1, 2, \ldots, 7$:

- Special Case 1 - Surface 1: { {1,0,1}, {0.4}, {1}, {1,1,0,1}}
- Special Case 2 - Surface 2: {{1,0,0.5}, {0.6}, {1}, {0.5,0.5,1,-1}}
- Special Case 3 - Surface 3: {{1,2,2}, {0.01}, {1}, {1.3,0.5,0.1,0.5}}
- Special Case 4 - Surface 4: {{0.2,1.8,3}, {0.1}, {0.7}, {0.6,0.7,1,1}}
- Special Case 5 - Surface 5: {{-1,0,-1}, {0}, {1}, {1,0.5,0,1}}

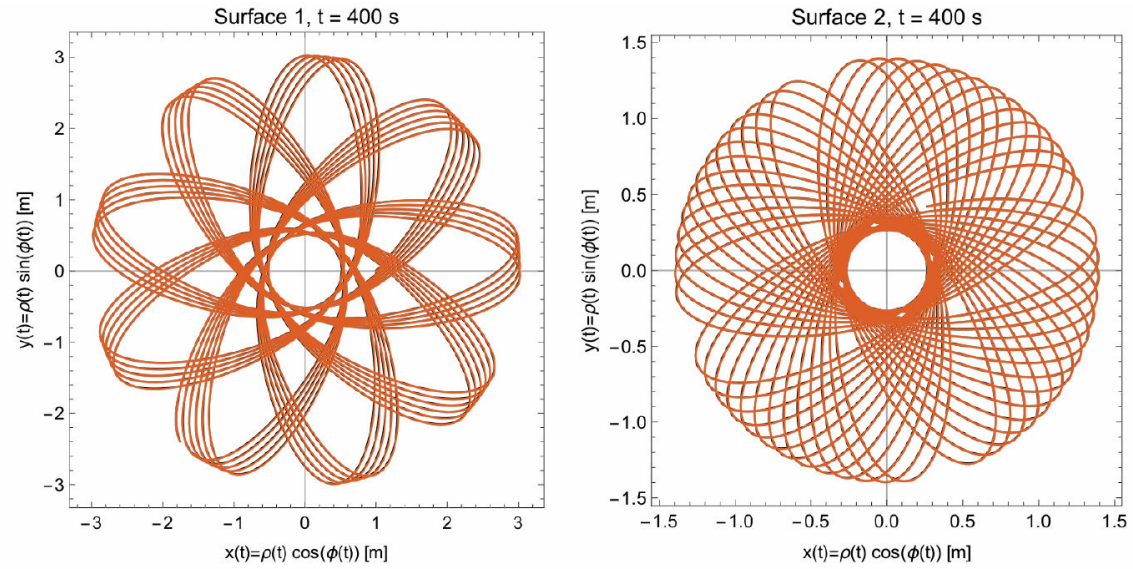

FIGURE 4. Parametric solutions for special cases 1 and 2 in the $x - y$ plane.

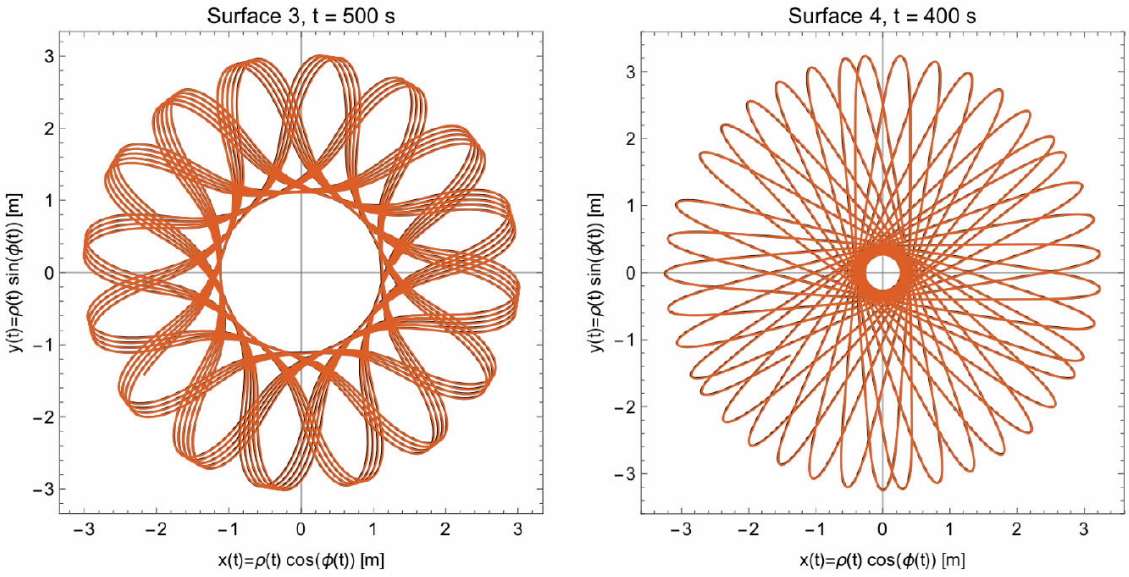

FIGURE 5. Parametric solutions for special cases 3 and 4 in the $x - y$ plane.

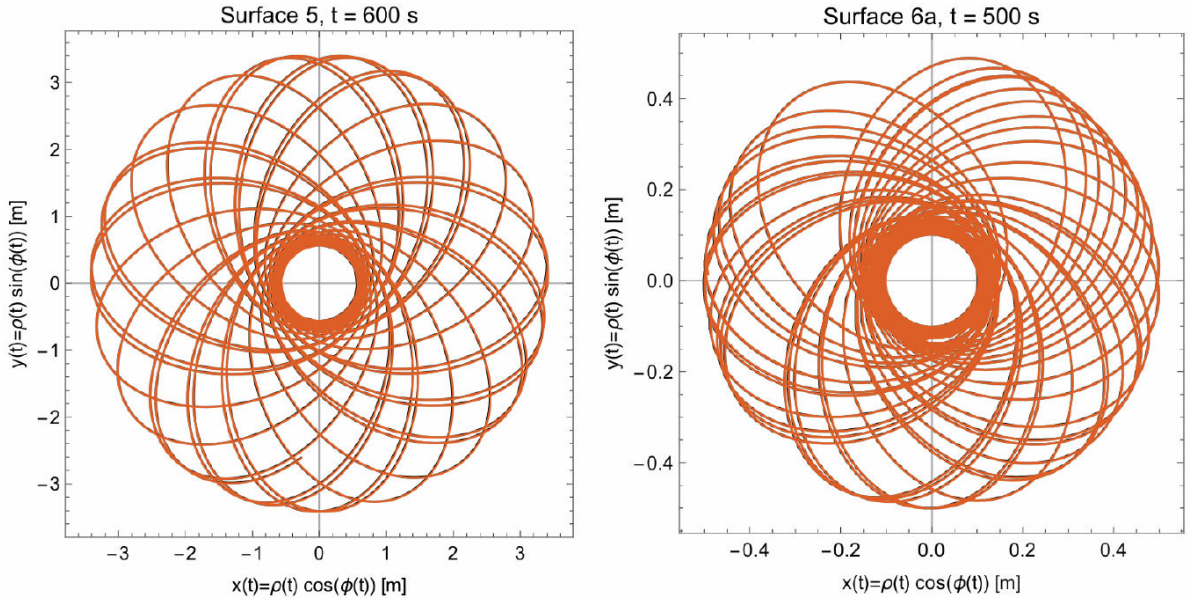

FIGURE 6. Parametric solutions for special cases 5 and 6 in the $x - y$ plane.

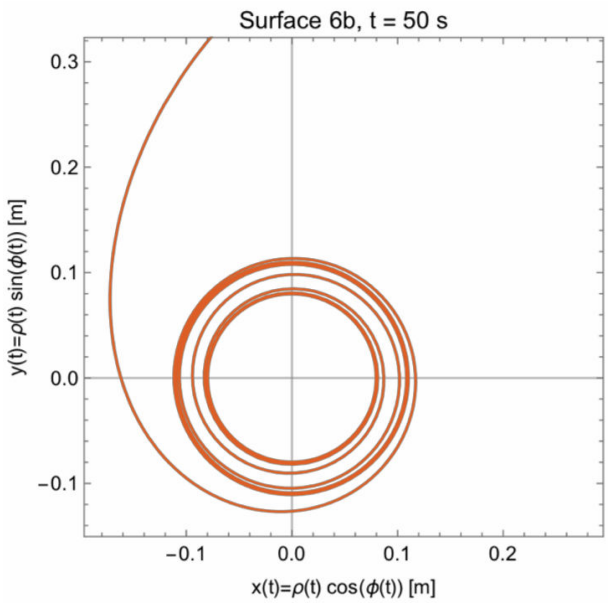

FIGURE 7. Parametric solution for special case 7 in the $x-y$ plane.

- Special Case 6 - Surface 6a: {{-0.1,0.08,-1/3}, {0.5}, {1}, {0.5,0,1,0.22600245}}
- Special Case 7 - Surface 6b: {{-0.1,0.08,-1/3}, {0.5}, {1}, {0.5,0,1,0.22600246}}.

This goal is achieved by using the technical computer software program *Wolfram Mathematica*, which is able to find a numeric solution for Eqs. (21), (22), and (23), when all the previous parameters are specified. The corresponding pieces of code used to solve these equations are shown in the Appendix. We proceed to show the solutions to the motion in the $x - y$ plane for each of these seven special cases.

2.2.1. *2D parametric plots*

The motion in the $x - y$ plane is presented for each jth special case in Figs. 4 – 7 evidencing the cyclic behavior of the system with stable orbits for cases 1, 2, 3, 4, 5, and 6. They also show that the motion takes place between some maximum and minimum values of ρ in the first six cases while it describes a monotonic (clockwise or anticlockwise) motion in the ϕ-coordinate. This last result is a consequence of the conservation of angular momentum described by Eq. (19), showing that $\dot{\phi}$ has always the same sign. Because of the non-decaying and cyclic motion of the sphere, it can be seen that there is no loss of energy in any trajectory, and thus, it satisfies the conditions set in its *Lagrangian* regarding the conservative nature of the constant gravitational field. To further analyze the motion presented for Surface 7, let us first observe the motion in its full three-dimensional nature in Figs. 8 to 14.

2.2.2. *3D parametric plots*

From these solutions to the equations of motion it can be seen that the holonomic constraints are satisfied by all the trajectories that the rolling sphere describes. Besides this, it can also be noticed that special case 7 has no stable orbits, but instead, its motion decays into circles of decreasing radius and its z-coordinate tends to minus infinity as time increases. Although each of the trajectories described by the sphere in special cases 6 and 7 are done over the same Surface 6, it can be seen that they are quite different since special case 6 has fully stable orbits just as the other previous five special cases while special case 7 does not.

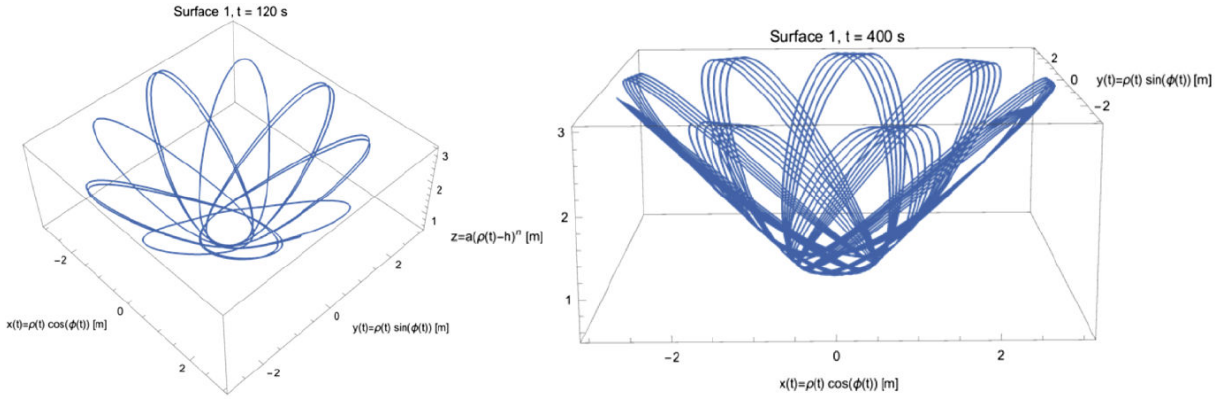

FIGURE 8. Three-dimensional parametric plot of the solution for Special Case 1.

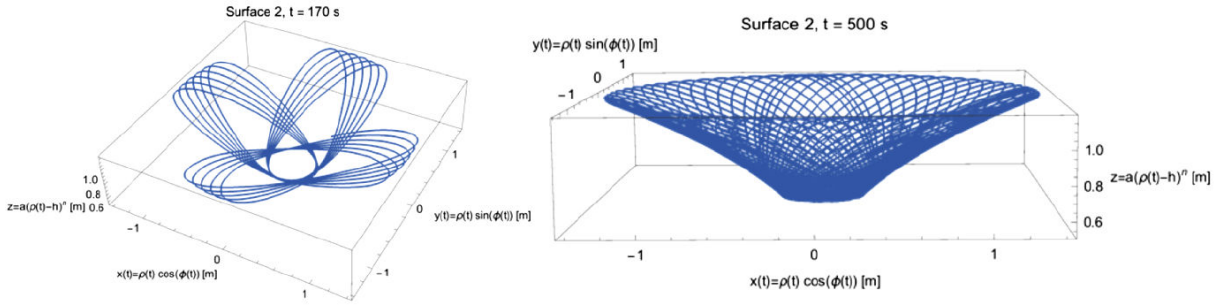

FIGURE 9. Three-dimensional parametric plot of the solution for Special Case 2.

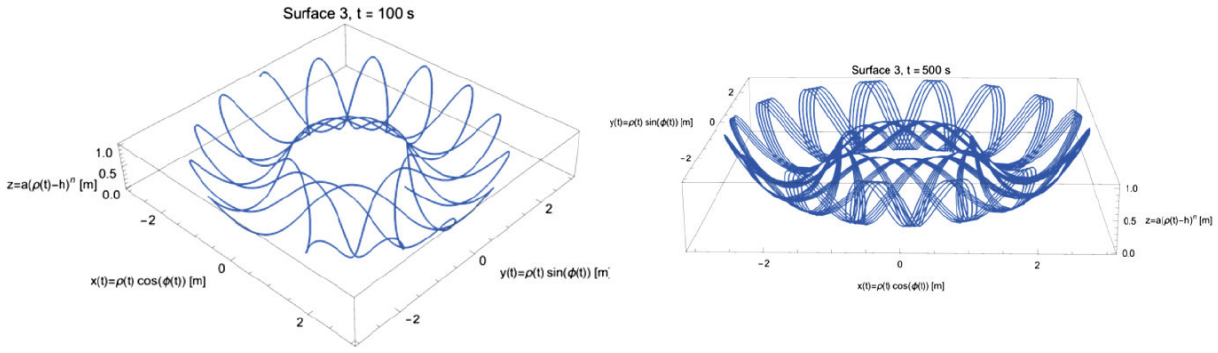

FIGURE 10. Three-dimensional parametric plot of the solution for Special Case 3.

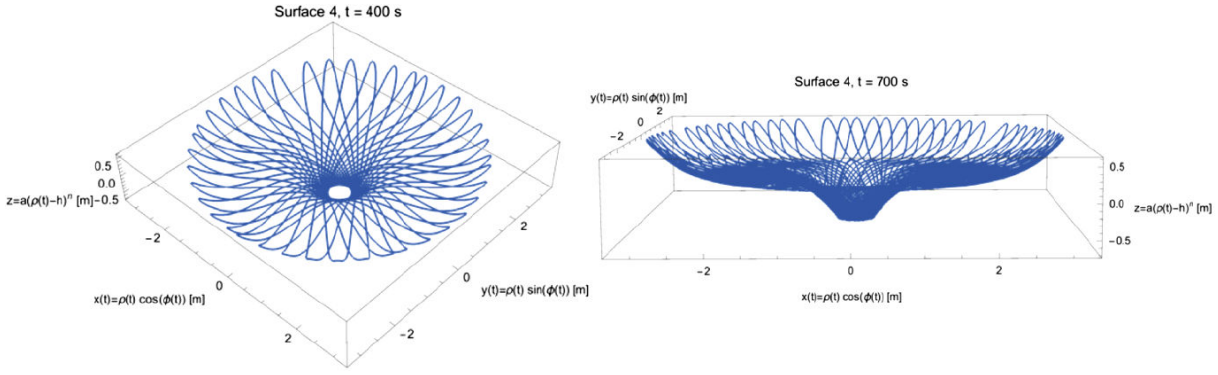

FIGURE 11. Three-dimensional parametric plot of the solution for Special Case 4.

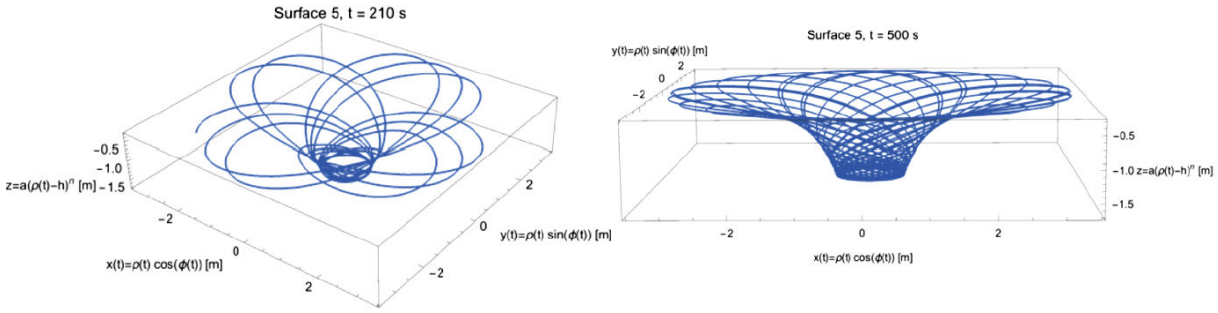

FIGURE 12. Three-dimensional parametric plot of the solution for Special Case 5.

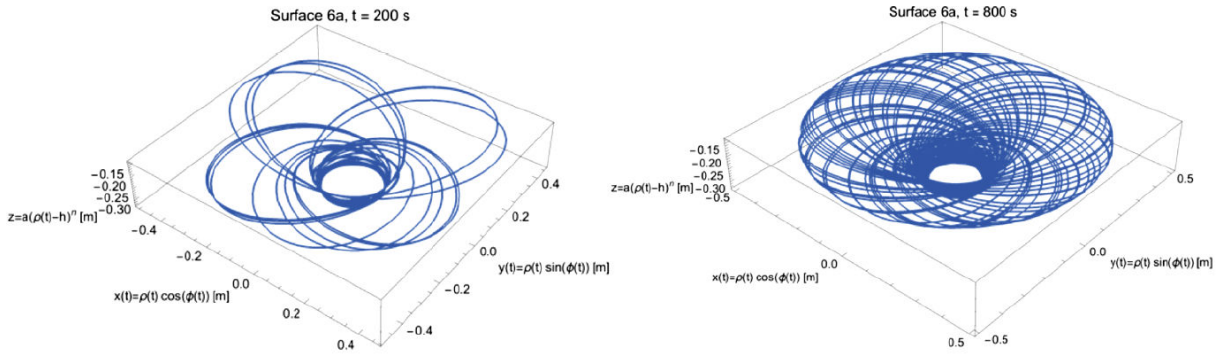

FIGURE 13. Three-dimensional parametric plot of the solution for Special Case 6.

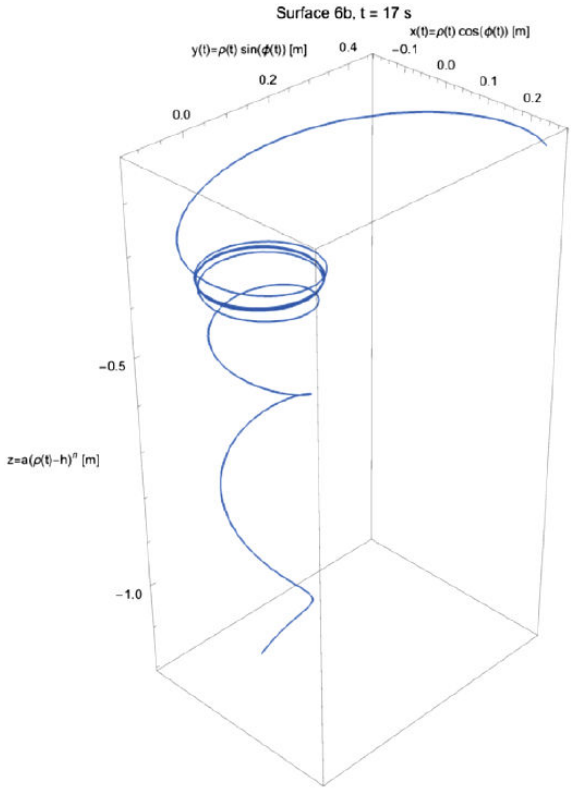

FIGURE 14. Three-dimensional parametric plot of the solution for Special Case 7.

This discrepancy in the motion is a result of the slight difference between the parameters given to each special case 6 and 7, which differ by 1×10^{-8} rad/s of their initial values for $\dot{\phi}(t)$, demonstrating that a relatively small change on the initial conditions may create a whole different outcome. It is also important to mention that the solutions that exhibit stable orbits show characteristic precession on them. Let us further analyze the motion of the rolling sphere by plotting the solution of its movement on the three cylindrical coordinates and their corresponding time derivatives as functions of time in Figs. 15 and 16.

2.2.3. Coordinates and speeds as functions of time

The motion in all three coordinates and their time-derivatives is found to describe a periodic behavior that is characteristic of the null loss of energy in the system. This statement holds just for the radial and azimuthal motions of special case 7, while an increasing and non-cyclic behavior is shown for the z-coordinate, which as was previously seen, with a slight change of initial conditions describes stable orbits. It is evident that certain asymptotic surfaces (like Surface 6) will exhibit non-cyclic motion on the z-coordinate under certain circumstances, since the motion of the sphere in these cases may approach to freefall as time tends to infinity.

The role of the conservation law Eq. (19) for the angular momentum is evidenced when comparing both the plot of the radial coordinate $\rho(t)$ and the plot of the angular speed $\dot{\phi}(t)$ as functions of time, for whenever the former is a minimum,

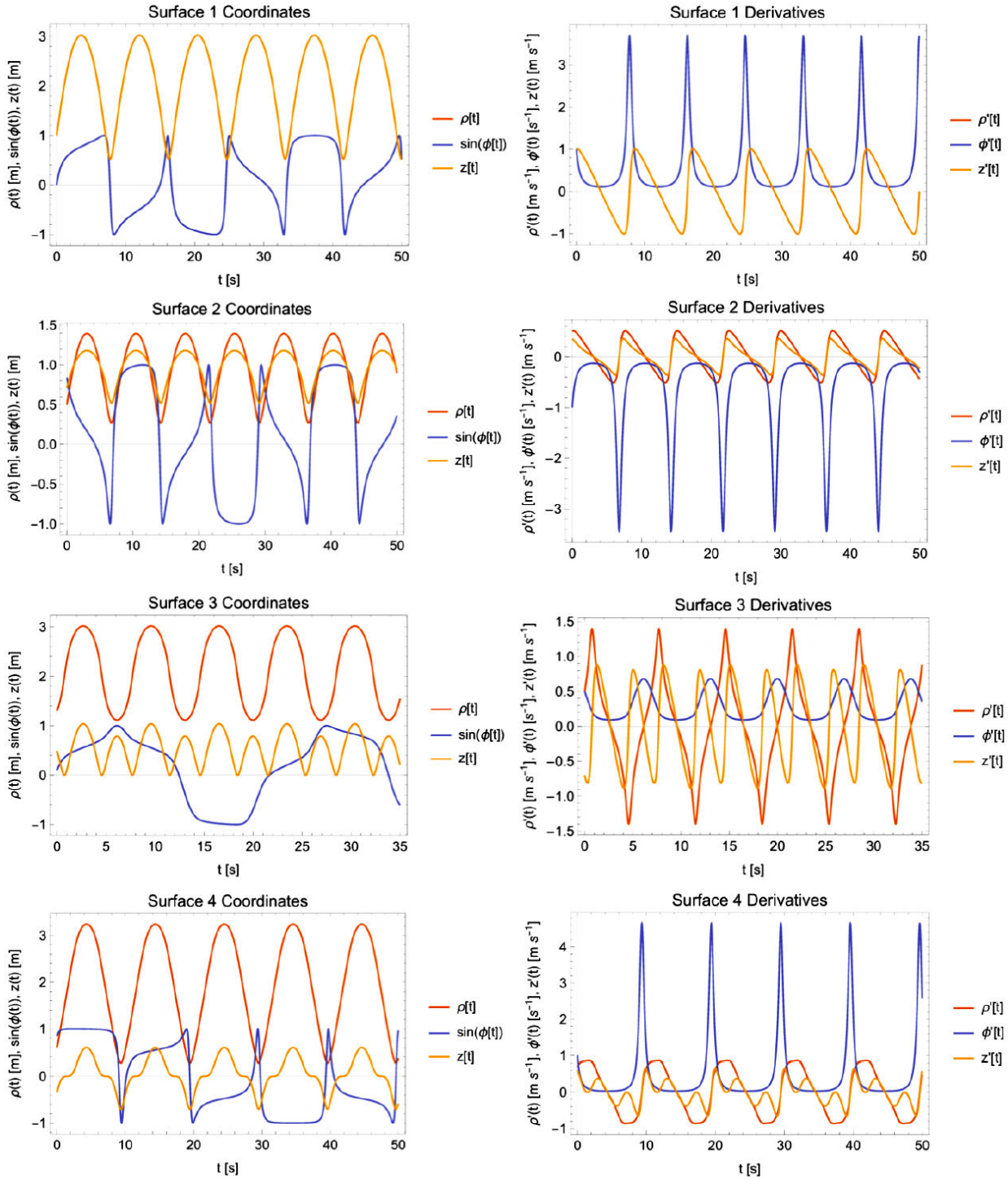

FIGURE 15. Plot of the solutions to the motion for the three coordinates and their time-derivatives as functions of time for special cases 1, 2, 3, and 4. For the sake of clarity, it was chosen not to plot $\phi(t)$ but instead $\sin(\phi(t))$. Nevertheless, such decision was arbitrary, so plotting $\cos(\phi(t))$ instead would have served the same purpose.

then the latter is a maximum, and vice versa. The symmetry of the motion of the sphere is not just a direct result of the azimuthal symmetry of the surface but also a consequence of the symmetry of the sphere itself, letting the motion repeat indefinitely for the cases in which stable orbits exist.

3. Approximation of an effective potential energy

By recalling the kinetic and potential energies (from the Lagrangian, in Eq. (13)) along with the conservation of the z-component of the sphere's angular momentum Eq. (19), we

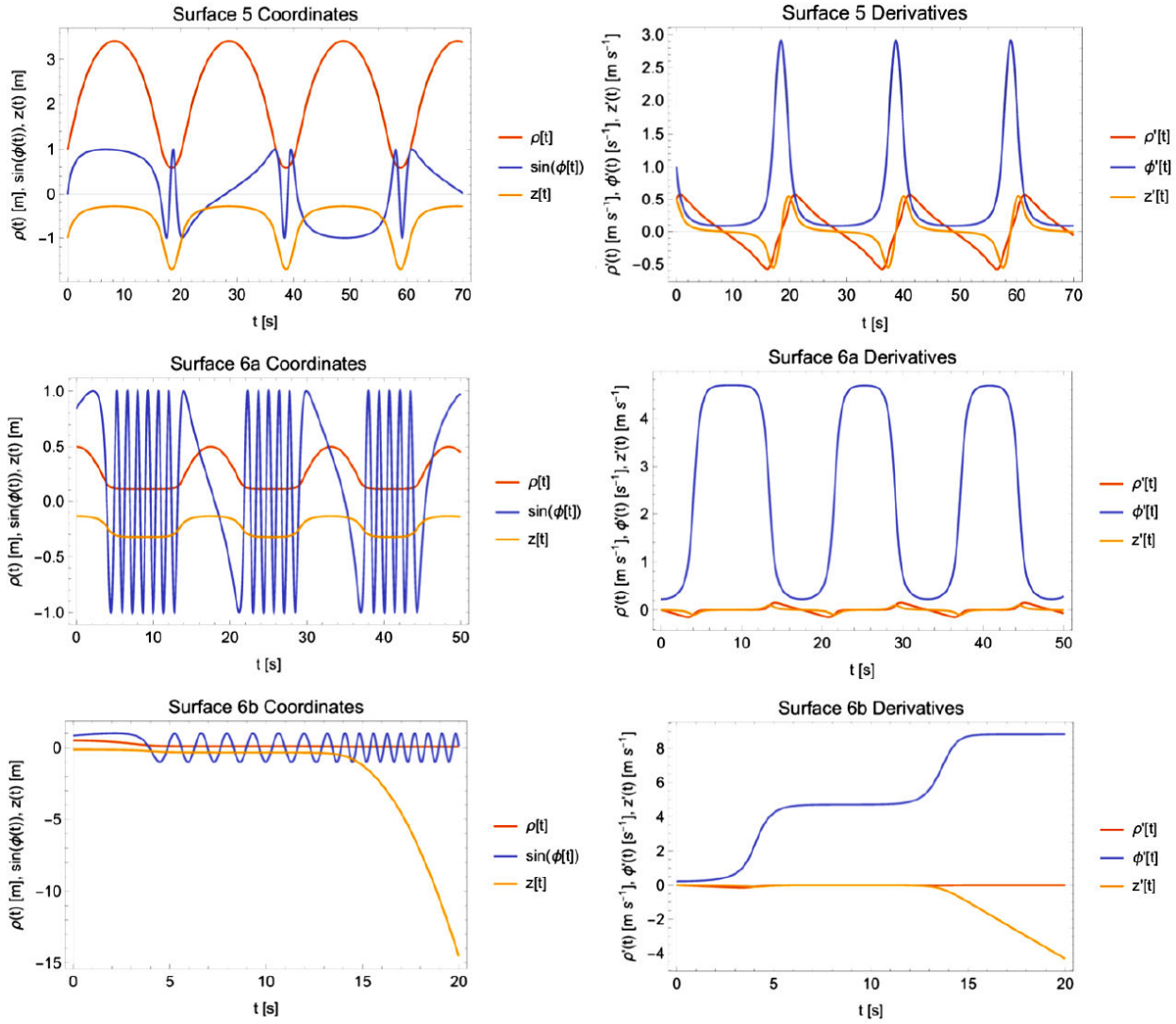

FIGURE 16. Plot of the solutions to the motion for the three coordinates and their time-derivatives as functions of time for Special Cases 5, 6, and 7.

can approximate an effective potential energy for certain special cases of the sphere's motion.

The total energy of the system is just the sum of its kinetic and potential energies:

$$E = T + V. \tag{24}$$

After substituting these energies from the Lagrangian (19) into (24) and expanding the first term we get:

$$\begin{aligned} E &= \frac{1}{2}m(1+k)\Big((1+a^2n^2(\rho-h)^{2(n-1)})\dot{\rho}^2+\rho^2\dot{\phi}^2\Big) \\ &\quad + amg(\rho-h)^n \\ E &= \frac{1}{2}m(1+k)(1+a^2n^2(\rho-h)^{2(n-1)})\dot{\rho}^2 \\ &\quad + \frac{1}{2}m(1+k)\rho^2\dot{\phi}^2 + amg(\rho-h)^n, \end{aligned} \tag{25}$$

where we can recognize the first and second terms as the radial and angular kinetic energies, respectively. Furthermore, by recalling that

$$L_z = m\rho^2\dot{\phi} = \text{constant}, \tag{26}$$

we can manipulate the angular kinetic energy term in the following way:

$$\begin{aligned} T_\phi \equiv \frac{1}{2}m(1+k)\rho^2\dot{\phi}^2 &= \frac{1}{2}(1+k)\frac{(m\rho^2\dot{\phi})^2}{m\rho^2} \\ &= \frac{1}{2}(1+k)\frac{L_z^2}{m\rho^2}. \end{aligned}$$

Therefore, by substituting this last result into the energy Eq. 25 we get:

$$E = \frac{1}{2}m(1+k)\left(1+a^2n^2(\rho-h)^{2(n-1)}\right)\dot{\rho}^2 + \frac{1}{2}(1+k)\frac{L_z^2}{m\rho^2} + amg(\rho-h)^n. \quad (27)$$

Notice that the last two terms depend only on the coordinate ρ in such a way that they could be merged into a unique effective potential energy for the system if the factor before $\dot{\rho}^2$ was just equal to one (since the first term would become dependent only of $\dot{\rho}$), which suggests that under the criterion that

$$a^2n^2(\rho-h)^{2(n-1)} \ll 1$$

or, because a^2n^2 is a positive quantity that can take any desired value

$$(\rho-h)^{2(n-1)} \ll \frac{1}{a^2n^2}, \quad (28)$$

then the energy equation for the rolling sphere becomes

$$E \approx \frac{1}{2}m(1+k)\dot{\rho}^2 + \frac{1}{2}(1+k)\frac{L_z^2}{m\rho^2} + amg(\rho-h)^n, \quad (29)$$

which can be rewritten in the following way

$$E = \frac{1}{2}m(1+k)\dot{\rho}^2 + V_{\text{eff}}(\rho), \quad (30)$$

with $V_{\text{eff}}(\rho)$ defined as:

$$V_{\text{eff}}(\rho) \equiv \frac{1}{2}(1+k)\frac{L_z^2}{m\rho^2} + amg(\rho-h)^n. \quad (31)$$

Equation (31) is the effective potential energy of the rolling sphere when its motion is governed under Eq. (28).

3.1. Gravitational well

When solving the famous "Two Body Problem" in classical gravitation, there is a common parameter called the "reduced mass" of two objects with masses m_1 and m_2, which is defined as [5]:

$$\mu = \frac{m_1m_2}{m_1+m_2}.$$

To make the following steps clearer, let us rename m_1 and m_2 as M and m, respectively. If we consider the case where $M \gg m$ and take the limit as M goes to infinity we get:

$$\lim_{M\to\infty}\mu = m.$$

This last result is important because the following cited equations use the parameter μ. This parameter will be shown as m since we will only be concerned with the case $M \gg m$ due to the following comparison. We can notice the similarity between Eq. (29) and the energy Eq. (32) for a particle of mass m moving under the presence of the gravitational field of a much larger mass M that satisfies the condition $M \gg m$ [6]:

$$E_G = \frac{1}{2}m\dot{\rho}^2 + \frac{1}{2}\frac{L_z^2}{m\rho^2} - \frac{GMm}{\rho}, \quad (32)$$

which has the corresponding effective potential energy function given by [1]

$$V_{\text{eff}}(\rho) = \frac{1}{2}\frac{L_z^2}{m\rho^2} - \frac{GMm}{\rho}.$$

Let us now recall the approximated energy equation for the rolling sphere:

$$E \cong \frac{1}{2}m(1+k)\dot{\rho}^2 + \frac{1}{2}(1+k)\frac{L_z^2}{m\rho^2} + amg(\rho-h)^n.$$

If our desire is to obtain a surface that generates an effective potential energy function for the rolling sphere similar to that one felt by the gravitationally-bound mass m under the condition $M \gg m$, we could just let $h = 0$, try to make k (from now on equal to cero) as small as possible, perhaps concentrating most of the sphere's mass into a small region compared to its radius in order to minimize its moment of inertia around any instantaneous rolling axis (and thus the constant k), and also let the following comparison between potential energies be:

$$amg\rho^n = -\frac{GMm}{\rho},$$
$$a\rho^n = -\left(\frac{GM}{g}\right)\frac{1}{\rho}, \quad (33)$$

where it can clearly be seen that a and n must take the following values:

$$a = -\left(\frac{GM}{g}\right), \quad n = -1.$$

The surface obtained by substituting these parameters into Eq. (3) is shown in Fig. 17.

The rolling object cannot be let to roll with any desired initial condition if we wish to obtain a similar motion to that of an object moving through the previously described gravitational field, for we must remember the criterion used to derive the effective potential (31) and the approximated energy Eq. (29). By substituting the last values for a and n into the Eq. (28) the criterion now becomes:

$$\rho \gg \sqrt{\frac{GM}{g}}. \quad (34)$$

This condition may be held if we recall that a particle that moves under a gravitational field with total energy $E < 0$ describes an elliptical orbit with its motion determined by the

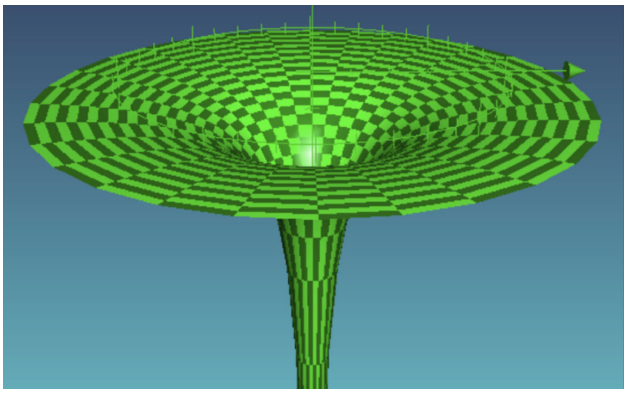

FIGURE 17. Surface 5 is the surface that mimics Newtonian gravitation under criterion in Eq. (30) (taking $GM/g = 1$ for demonstration purposes).

following set of equations [7,8]:

$$\rho_{\min} = a'(1-e) \tag{35}$$

$$E = -\frac{GMm}{2a'} \tag{36}$$

$$e = \sqrt{1 + \frac{2EL_Z^2}{G^2M^2m^3}} \tag{37}$$

$$L_Z = m\rho(0)^2\dot{\phi}(0) \tag{38}$$

$$E_G = \frac{1}{2}m(\dot{\rho}(0)^2 + \rho(0)^2\dot{\phi}(0)^2) - \frac{GMm}{\rho(0)}, \tag{39}$$

where a' is the semimajor axis of the elliptical orbit, e is its eccentricity (both constants determining the geometry of the orbit), L_Z is the angular momentum around the z-axis (which is taken to cross one focus and be perpendicular to the plane of motion of the particle), and E_G is the total mechanical energy of the particle. Both of these last quantities - L_Z and E_G- are conserved; the former as a result from Kepler's Second Law, and the latter as a consequence of the conservative nature of the gravitational field.

Moreover, by substituting Eqs. (36) and (37) into the Eq. (35) for the orbit's periapsis $\rho_{\min}$, using this quantity in criterion (34) (for it represents the closest distance between the object and the origin of our coordinate system), and introducing an arbitrary new constant l to change the inequality into an equation (which results in an increasing accuracy of the model with an increasing value of l) we get:

$$\rho_{\min} = -\frac{GMm}{2E}\left(1 - \sqrt{1 + \frac{2EL_Z^2}{G^2M^2m^3}}\right) \equiv l\sqrt{\frac{GM}{g}}. \tag{40}$$

By substituting Eqs. (38) and (39) into this last Eq. (40) we obtain the following relationship between the initial conditions $\rho(0)$, $\dot{\rho}(0)$, and $\dot{\phi}(0)$:

$$\rho_{\min} = -\frac{GM}{\dot{\rho}(0)^2 + \rho(0)^2\dot{\phi}(0)^2 - \frac{2GM}{\rho(0)}} \times \left(1 - \sqrt{1 + \frac{\rho(0)^4\dot{\phi}(0)^2\left(\dot{\rho}(0)^2 + \rho(0)^2\dot{\phi}(0)^2 - \frac{2GM}{\rho(0)}\right)}{G^2M^2}}\right) = l\sqrt{\frac{GM}{g}}. \tag{41}$$

We also get the natural result that this last equation is independent of the sphere's mass m and the value of $\phi(0)$, for the last one just rotates the resulting ellipse in the counterclockwise direction for increasing initial values of $\phi(0)$ [9], and the first one shows the analogy with classical gravitation where, under the condition $M \gg m$, the object's orbit is independent of its own mass. On the other hand, we may solve this equation by choosing the value of any desired two variables $\rho(0)$, $\dot{\rho}(0)$, or $\dot{\phi}(0)$ and using mathematical software to solve for the third.

It is also evident that the criterion

$$\rho(0) > l\sqrt{\frac{GM}{g}} \tag{42}$$

must always be met; for $\rho(0)$ should never be smaller than $\rho_{\min}$, which is by definition the smallest distance from the orbiting mass m to the much larger mass M, or in other words, the periapsis of the sphere's elliptical orbit. Because our desire is to obtain elliptical orbits, there's another condition that must be satisfied by $\rho(0)$, $\dot{\rho}(0)$, and $\dot{\phi}(0)$:

$$E_G = \frac{1}{2}m(\dot{\rho}(0)^2 + \rho(0)^2\dot{\phi}(0)^2) - \frac{GMm}{\rho(0)} < 0. \tag{43}$$

If a certain value of $\rho(0)$ that satisfies (42) is given, then the values of $\dot{\rho}(0)$ and $\dot{\phi}(0)$ that will also satisfy the energy inequality (43) and Eq. (41) can be determined by using mathematical software. Let us proceed to observe some examples of the solutions to Eqs. (21) and (22) when the sphere rolls over Surface 5, under criterion (34), and thus, with its initial conditions satisfying the relationships (41), (42) and (43) in Figs. 18 and 19.

These solutions to the motion seem to describe elliptical orbits as those performed by astronomical objects around a relatively massive star, each with different initial conditions that satisfy relationships (41), (42) and (43). It is important to remember that these orbits are just approximately elliptical, if we let the sphere orbit for enough time, this approximated model will no longer be accurate and the motion will stop describing perfectly elliptical orbits, as is the case of the "Elliptic" Orbit 6 shown in Fig. 19. It is also worth comparing these trajectories to those followed by the sphere in Special Case 5 (shown in Figs. 6 and 12), where it also rolls over

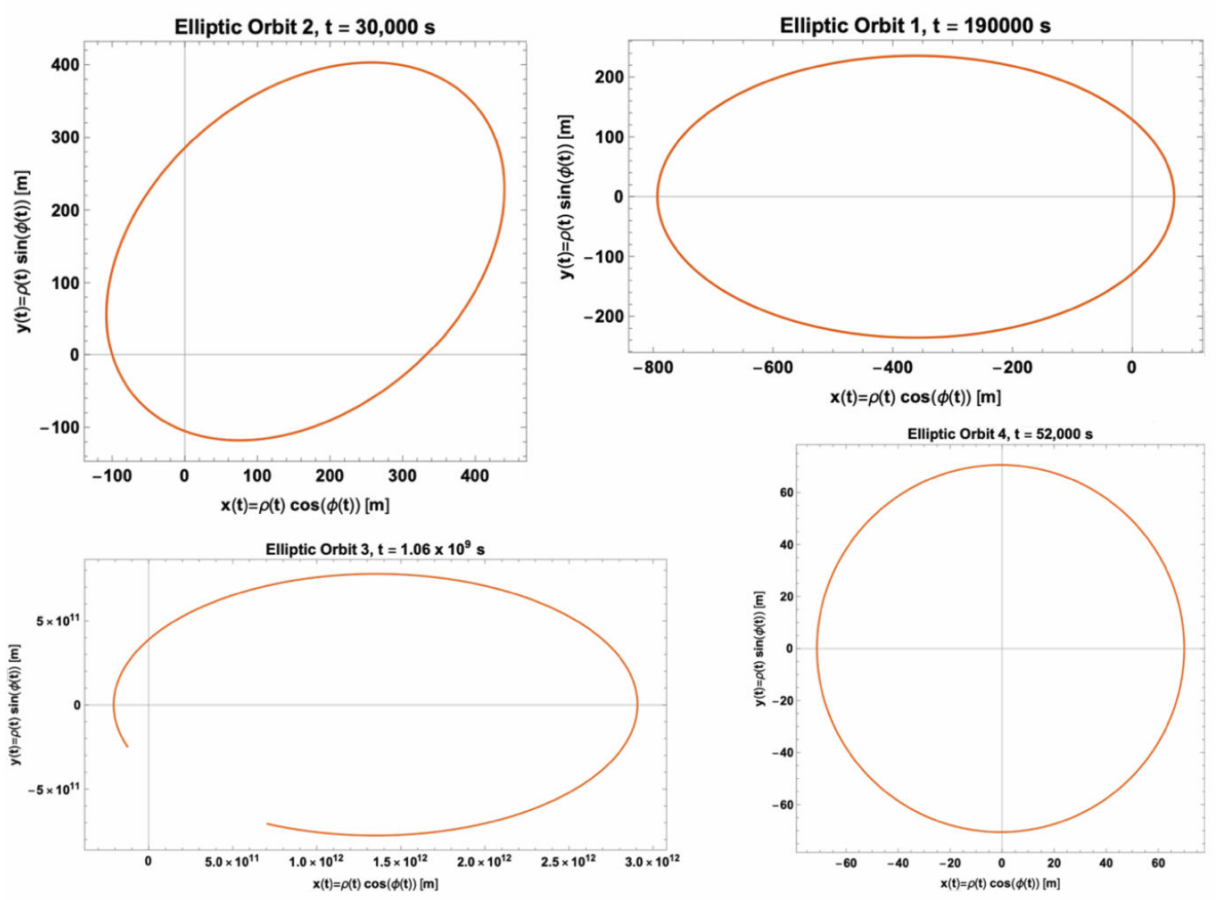

FIGURE 18. Parametric solutions for the movement of the sphere on Surface 5 and under the previous conditions, describing elliptical orbits. The following are the parameters G, M, g, l, $\rho(0)$, $\phi(0)$, $\dot{\rho}(0)$, and $\dot{\phi}(0)$ used to create these graphs, all of them in their respective MKS units. Orbit 1: (1, 1, 1, 70, 70, 0, 0, 0.00231473), orbit 2: (1, 1, 1, 90, 100, π, 0.0372136, -0.00124006), orbit 3: (6×10^{-11}, 2×10^{-30}, 10, 60, 1×10^{12}, $-\pi/4$, 10788.3, 6.82306×10^{-9}) [parameters comparable with the ones from planets in our solar system], orbit 4: (1, 1, 1, 70, 70, 0, 0, 0.00171473).

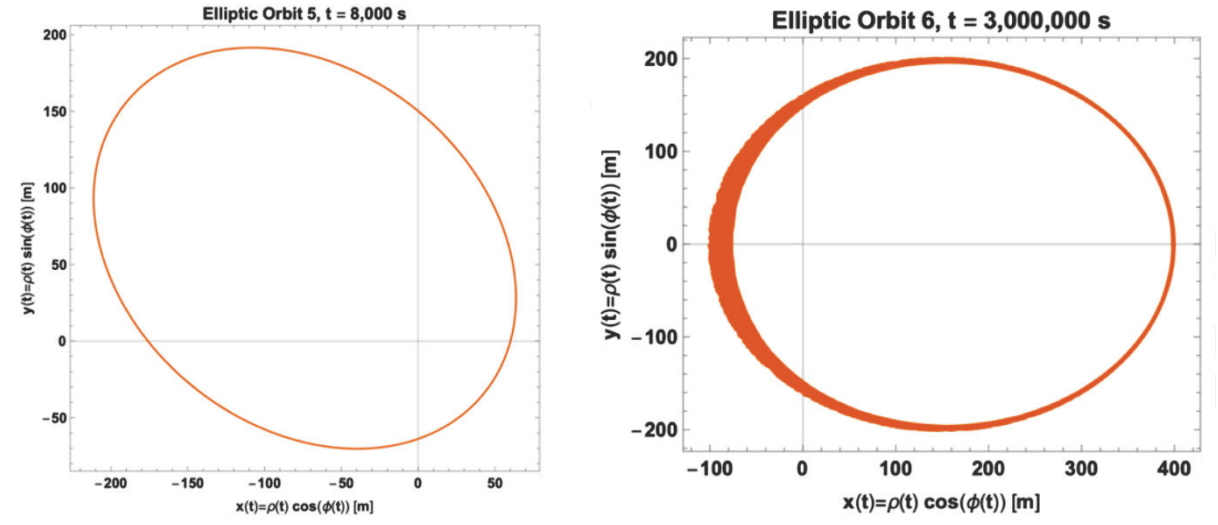

FIGURE 19. Parametric solutions for the movement of the sphere on Surface 5 and under the previous conditions, describing elliptical orbits. The following are the parameters G, M, g, l, $\rho(0)$, $\phi(0)$, $\dot{\rho}(0)$, and $\dot{\phi}(0)$ used to create these graphs, all of them with their respective MKS units. Orbit 5: (4, 3, 10, 50, 100, $\pi/3$, 0.229464, 0.00327871), orbit 6: (2,1,1,70,400,0,0,0.000111352).

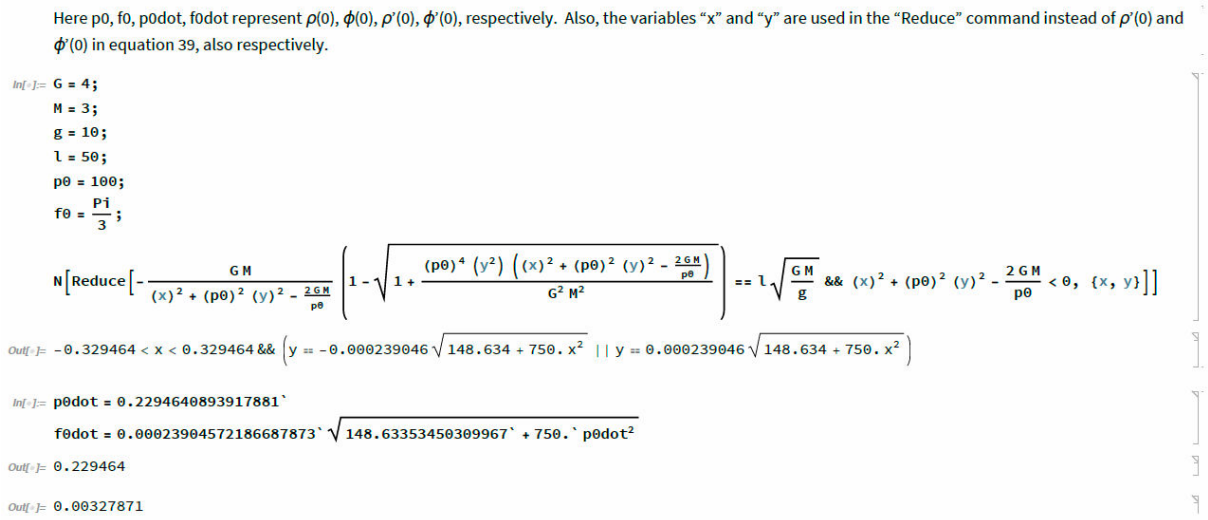

FIGURE 20. Code used in *Wolfram Mathematica* to obtain the initial conditions required to produce Elliptic Orbit 5, a similar procedure was used for creating the other five elliptic orbits.

Surface 5 but without describing elliptical orbits, evidencing that its initial conditions do not satisfy Eq. (41).

The code used in *Wolfram Mathematica* to solve the system of relations (41) and (43) that determines the values that $\dot{\rho}(0)$ and $\dot{\phi}(0)$ can take for a given initial radial condition $\rho(0)$ is shown with the specific example of Elliptic Orbit 5 in Fig. 20. After obtaining the possible values for $\dot{\rho}(0)$ and $\dot{\phi}(0)$, any value within the output range for $\dot{\rho}(0)$ can be selected, automatically determining the values that $\dot{\phi}(0)$ can take to satisfy the conditions (41) and (43), one positive and one negative with same modulus, demonstrating once again the presence of the azimuthal symmetry of the system.

4. Modelling with friction

4.1. Introduction of friction into the Lagrangian

The previous model (the one described by Eqs. (21), (22), and (23) is not accurate when considering the presence of non-conservative forces as friction. If we assume that the rolling-without-slipping condition takes place, we can notice that "no loss of mechanical energy occurs [due to friction between the sphere and the surface] because the contact point is at rest relative to the surface at any instant" since this is part of the definition of the rolling-without-slipping condition [10]. Therefore, under this idealistic condition, we would just have to concern about the friction that the rolling sphere experiences with air if it is our wish to describe the motion of the sphere under these circumstances.

Let us consider a force of friction between the sphere and the air as a function of the rolling object's speed with the following form:

$$\vec{F} = -(c_1|\vec{v}| + c_2|\vec{v}|^2 + \ldots + c_N|\vec{v}|^N)\hat{v} = -\left(\sum_{k=1}^{N} c_k|\vec{v}|^k\right)\hat{v} = -\psi(|\vec{v}|)\hat{v}, \tag{44}$$

where:

$$\psi(|\hat{v}|) \equiv \left(\sum_{k=1}^{N} c_k|\vec{v}|^k\right).$$

It is considered that friction between air and the sphere takes this form since "any reasonable function is expected to have a Taylor series expansion, $F = a + bv + cv^2 + \ldots$. For low enough v, the first three terms should give a good approximation, and, since $F = 0$ when $v = 0$ the constant term, a, has to be zero" [1]. Therefore there is no need to consider a constant c_0 in Eq. (44). Likewise, with the objective of not losing generality, a "full" (N-terms) power series expansion of the friction force is considered in the following process.

According to Goldstein, "if not all the forces acting on the system are derivable from a potential, then Lagrange's equations can always be written in the form" [11]

$$\frac{d}{dt}\left(\frac{\partial \mathcal{L}}{\partial \dot{q}_i}\right) - \frac{\partial \mathcal{L}}{\partial q_i} - Q_i = 0, \tag{45}$$

with Q_i defined as:

$$Q_i \equiv \vec{F} \cdot \frac{\partial \vec{v}}{\partial \dot{q}_i} = -\psi(|\vec{v}|)\frac{\partial |\vec{v}|}{\partial \dot{q}_i}, \tag{46}$$

where in the last step Eq. (44) has been used. By recalling the Eq. (11) for the sphere's squared speed in cylindrical coordinates, we have:

$$|\vec{v}|^2 = (1 + a^2n^2(\rho - h)^{2(n-1)})\dot{\rho}^2 + \rho^2\dot{\phi}^2 \equiv w_1\dot{q}_1^2 + w_2\dot{q}_2^2, \tag{47}$$

with:

$$w_1 \equiv (1 + a^2 n^2 (\rho - h)^{2(n-1)})$$
$$w_2 \equiv \rho^2.$$

And by calculating the derivative of (47) with respect to $\dot{q}_i$, with $i \in \{1, 2\}$, we get:

$$\frac{\partial |\vec{v}|}{\partial \dot{q}_i} = w_i \frac{\dot{q}_i}{|\vec{v}|}.$$

Likewise, by substituting this last result into Eq. (46) we get:

$$Q_i = -\psi(|\vec{v}|)\frac{\partial \vec{v}}{\partial \dot{q}_i} = -\left(\sum_{k=1}^{N} c_k |\vec{v}|^k\right) w_i \frac{\dot{q}_i}{|\vec{v}|}$$
$$= -\left(\sum_{k=1}^{N} c_k |\vec{v}|^{k-1}\right) w_i \dot{q}_i. \quad (48)$$

Therefore the Euler-Lagrange Eq. (45) for the *i*-th coordinate is:

$$\frac{d}{dt}\left(\frac{\partial \mathcal{L}}{\partial \dot{q}_i}\right) - \frac{\partial \mathcal{L}}{\partial q_i} + \left(\sum_{k=1}^{N} c_k |\vec{v}|^{k-1}\right) w_i \dot{q}_i = 0. \quad (49)$$

And now by substituting Eqs. (14) and (47) into (49) for the ρ and ϕ-coordinates, as well as for the *i*-th constants, we get the equations of motion (50) and (51), which along with Eq. (52), let us once again determine the full translational motion of the sphere but now under the presence of a force of friction as described by Eq. (44):

$$m(1+k)\Big[(1 + a^2 n^2 (\rho - h)^{2(n-1)})\ddot{\rho} + a^2 n^2 (n-1)(\rho - h)^{2n-3}\dot{\rho}^2 - \rho\dot{\phi}^2 + \frac{ang(\rho - h)^{n-1}}{(1+k)}\Big] + \left(\sum_{k=1}^{N} c_k |\vec{v}|^{k-1}\right) \times (1 + a^2 n^2 (\rho - h)^{2(n-1)})\dot{\rho} = 0 \quad (50)$$

$$m(1+k)\left[\rho^2\ddot{\phi} + 2\rho\dot{\rho}\dot{\phi}\right] + \left(\sum_{k=1}^{N} c_k |\vec{v}|^{k-1}\right)\rho^2\dot{\phi} = 0 \quad (51)$$

$$z = a(\rho - h)^n. \quad (52)$$

In analogy with part one, this system of nonlinear coupled ordinary differential equations can be numerically solved by specifying each of the following parameters:

- Three surface constants: a, n, h.
- Two rigid body parameters: m, k
- N friction constants: $c_1, c_2, \ldots c_N$
- Four initial conditions: $\rho(0)$, $\dot{\rho}(0)$, $\phi(0)$, and $\dot{\phi}(0)$.

4.2. Analysis of Special Cases with Friction

4.2.1. 2D parametric plots

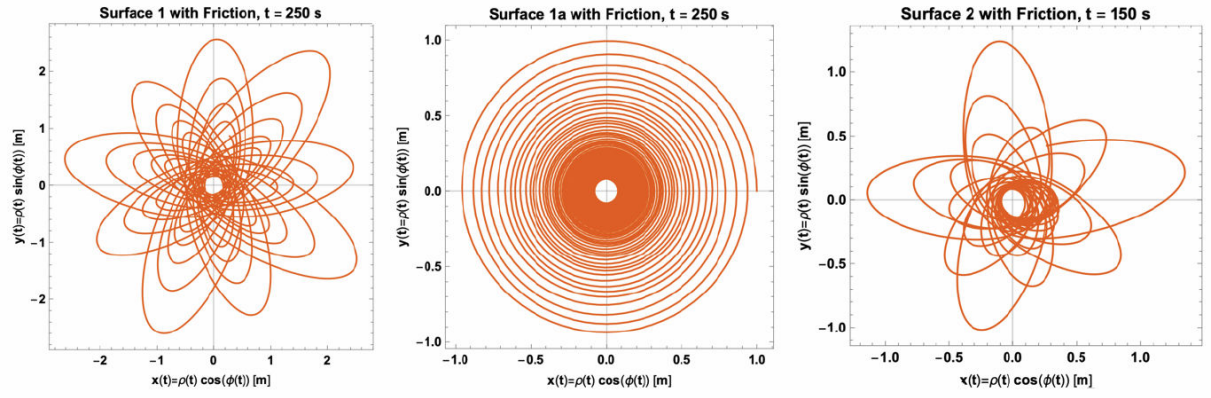

FIGURE 21. Parametric solutions in the $x - y$ plane for special cases 1 and 2 with friction. The plot for Surface 1a was made with the same parameters as Special Case 1 but with $k = 0.01$ and $\dot{\rho}(0) = 0$, which in the absence of friction, would create an almost-circular orbit.

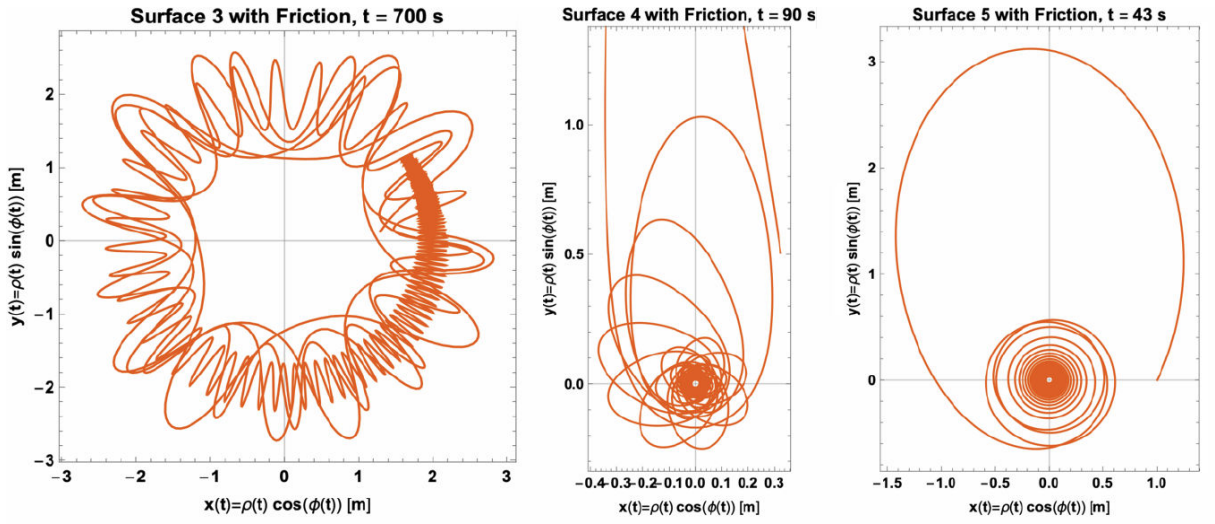

FIGURE 22. Parametric solutions in the $x - y$ plane for special cases 3, 4, and 5 with friction.

4.2.2. 3D parametric plots

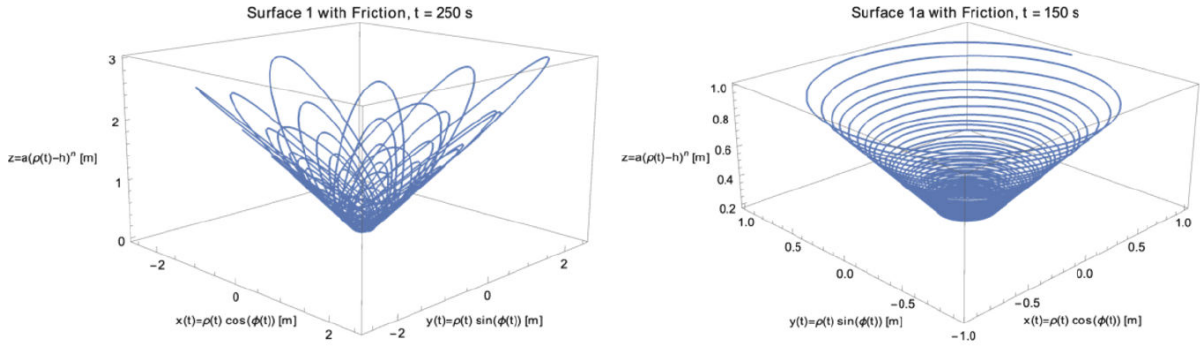

FIGURE 23. Three-dimensional parametric plots of the solutions for the special case 1 and for Surface 1a with friction.

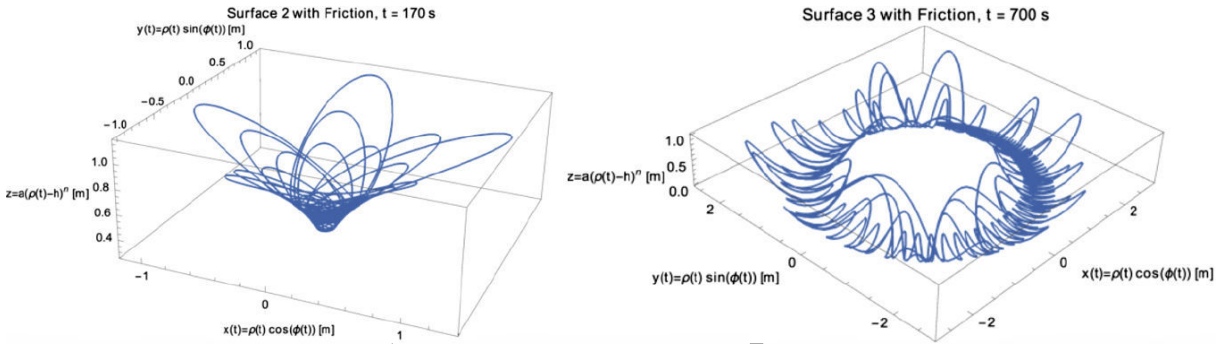

FIGURE 24. Three-dimensional parametric plots of the solutions for special cases 2 and 3 with friction.

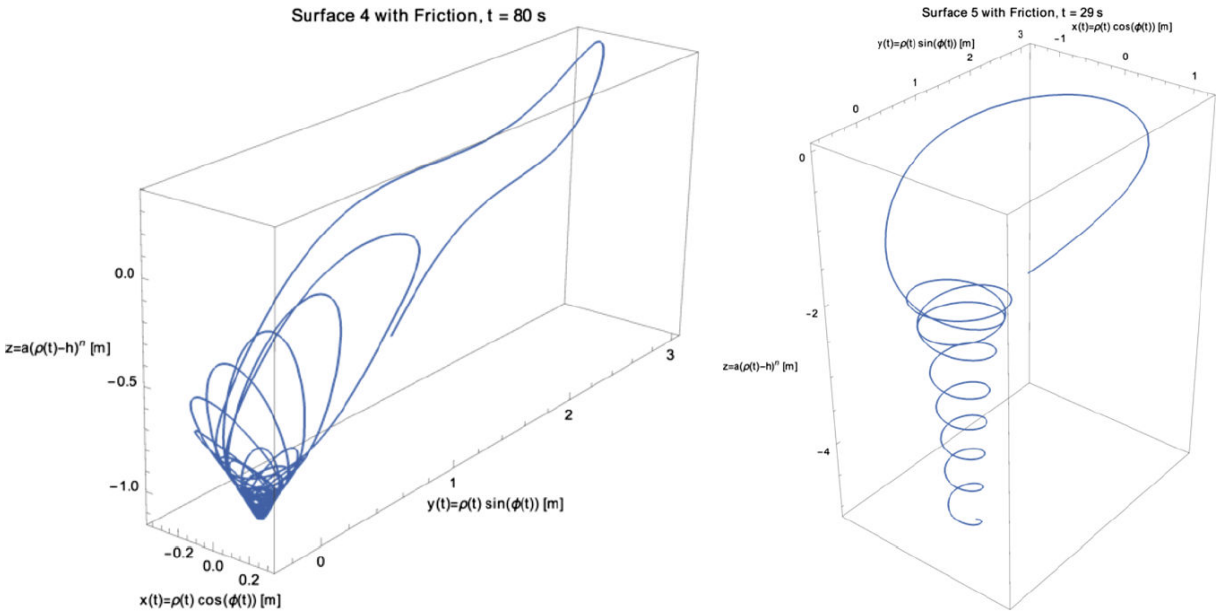

FIGURE 25. Three-dimensional parametric plots of the solutions for special cases 4 and 5 with friction.

4.2.3. *Coordinates and speeds as functions of time*

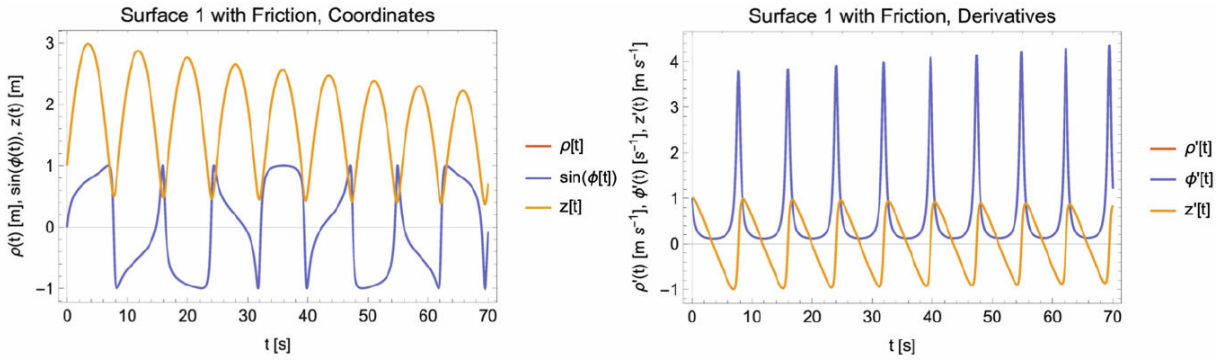

FIGURE 26. Plot of the motion in the three cylindrical coordinates and their corresponding time-derivatives as functions of time for special case 1.

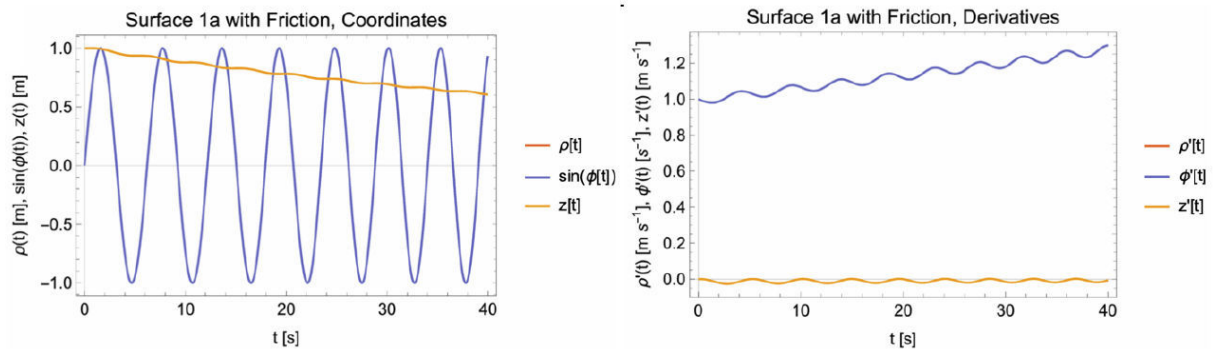

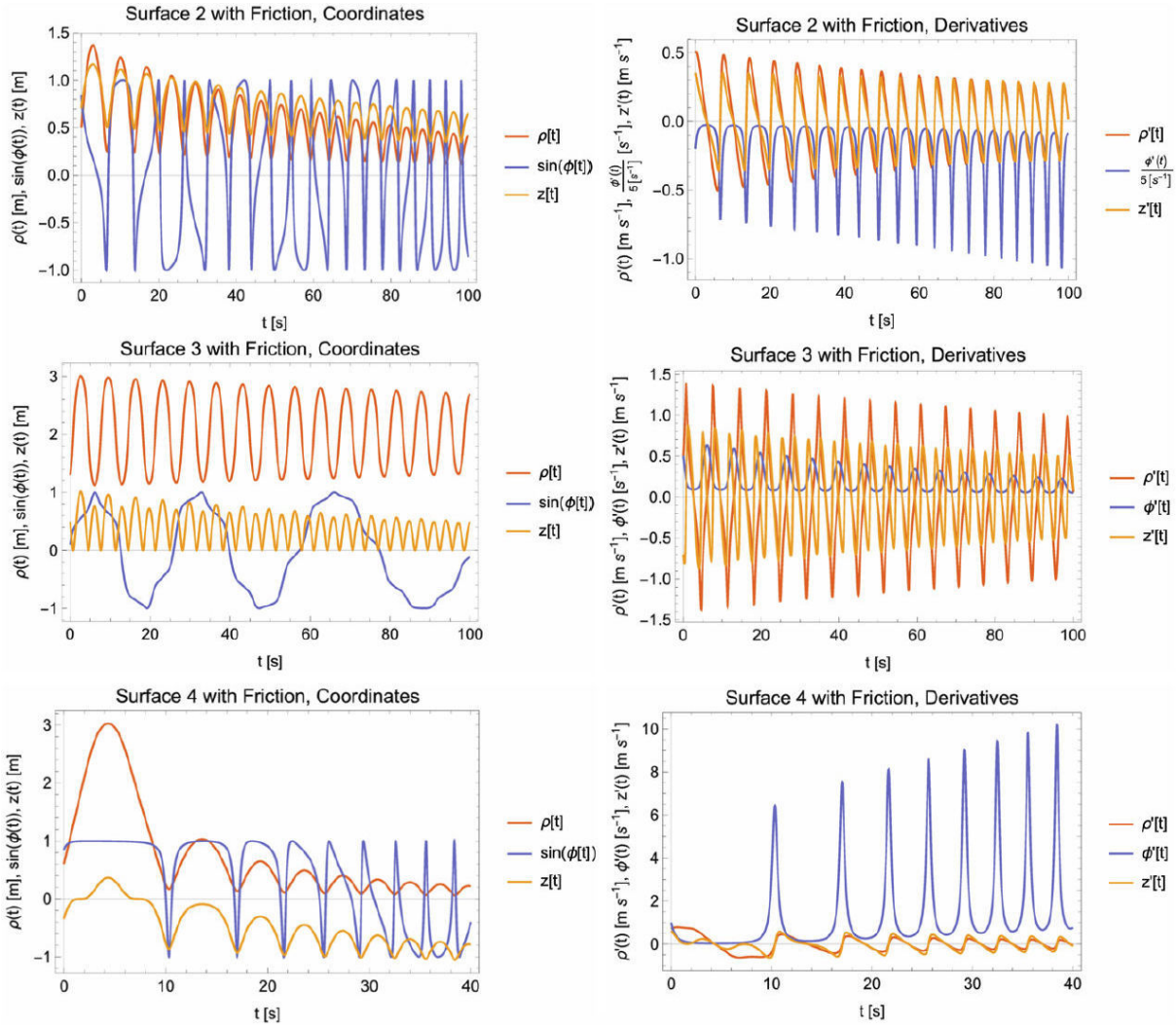

FIGURE 27. Plot of the motion in the three cylindrical coordinates and their corresponding time-derivatives as functions of time for Surface 1a and special cases 2, 3, and 4.

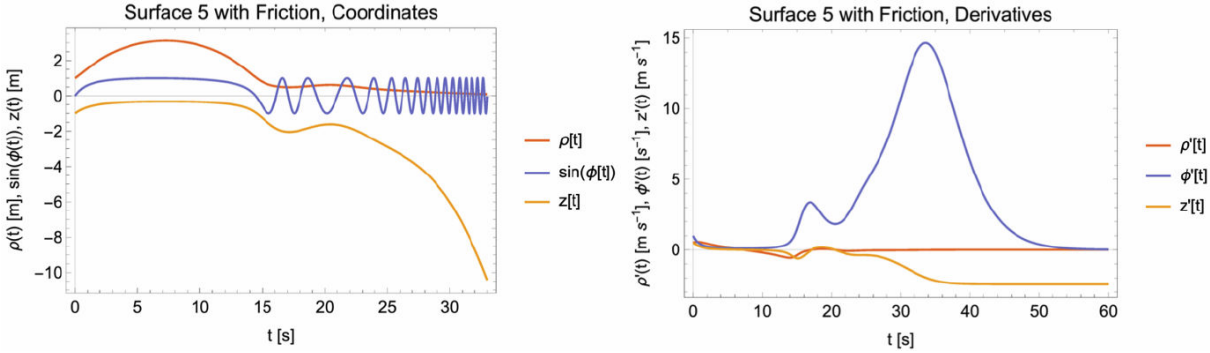

FIGURE 28. Plot of the motion in the three cylindrical coordinates and their corresponding-time derivatives as functions of time for special case 5.

4.2.4. Energies as functions of time

The previous solutions to the motion of the sphere were numerically solved with *Wolfram Mathematica* by specifying the same parameters as in the Special Cases analyzed in Part 1, plus the new special case for Surface 1a where the same parameters as special case 1 were used except for those specified in Fig. 21's caption. Different values for N and the c_k coefficients in Eqs. (50) and (51) were selected for each case to show the behavior of the system under arbitrarily different

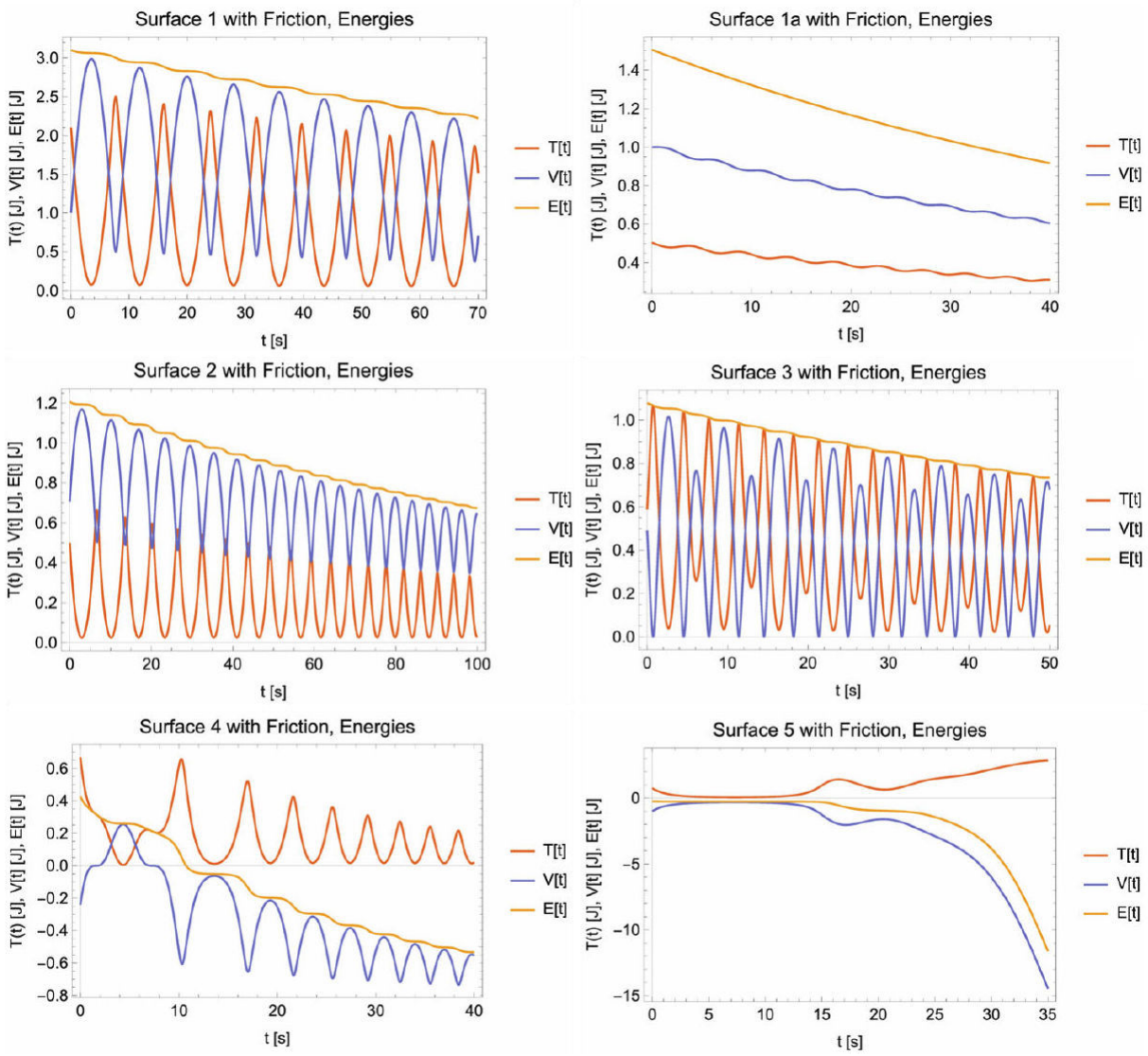

FIGURE 29. Plot of the dependence of the Kinetic $T(t)$ (Eq. 9), Potential $V(t)$ (Eq. 5), and Total Mechanical $E(t) = T(t) + V(t)$ energies as functions of time for special cases 1, 2, 3, 4, 5, and Surface 1a with friction.

forces of friction. These equations may take as input any desired value for such quantities, resulting in different but corresponding solutions to the motion as determined by Eqs. (50), (51) and (52). Each c_k has its corresponding unit kg m^{1-k} s^{k-2}.

Friction Parameters:

- Special Case 1 - Surface: $c_1 = 0.01$
- N/A - Surface 1a: $c_1 = 0.01$, $c_2 = 0.01$
- Special Case 2 - Surface 2: $c_1 = 0.01$, $c_2 = 0.02$
- Special Case 3 - Surface 3: $c_1 = 0.08$
- Special Case 4 - Surface 4: $c_1 = 0.040$, $c_2 = 0.030$, $c_3 = 0.020$. $c_4 = 0.010$
- Special Case 5 - Surface 5: $c_1 = 0.001$, $c_2 = 0.001$, $c_3 = 0.002$, $c_4 = 0.002$, $c_5 = 0.003$, $c_6 = 0.003$.

The effect of the loss of kinetic and potential energy in the system can clearly be seen in the 2D and 3D Parametric Plots of the motion shown in Figs. 21 to 25, both by the decrease of the orbits' radius and/or the following stationary motion that is obtained from non-asymptotic surfaces. This can intuitively (although of course not necessarily) indicate that the equations of motion obtained are in agreement with reality when the sphere is directly experiencing a friction force as described by Eq. 44. It can also be observed that the motion effectively stops in a potential valley when there is one -like with Surface 3 in special case 3- while losing kinetic energy and speed in both the radial and angular coordinates.

Furthermore, the plot of the coordinates and their time derivatives as functions of time in Figs. 26, 27 and 28, reveal that the cyclic behavior of the sphere is deformed by

the presence of friction, reducing or augmenting the amplitude of the oscillations that these functions exhibit, as well as stretching or compressing them along the t-axis when they are plotted against time. From the energy graphs shown in Fig. 29 it can be observed that the total mechanical energy of the system decreases invariably as time goes by and as a direct consequence of the energy dissipation that originates from friction. Besides this, it is also worth noting the different outcomes that Eqs. (50) and (51) predict for special case 5 (on the asymptotic Surface 5), where the sphere falls to ever-decreasing negative z-values as shown in Figs. 22 and 25 with the same conditions that in the frictionless case would make the sphere describe stable orbits as shown in Figs. 6 and 12.

The plot of speeds against time for this last case in Fig. 28 reveals the important prediction that the sphere must reach a terminal z-coordinate-speed as it falls with aerodynamic friction, as well as an asymptotic behavior to cero for the speed in the ρ and ϕ-coordinates. It is also worth noting that Eqs. (50) and (51) are dependent on the mass m of the sphere unless all their friction coefficients equal cero, where the equations become independent of *m* once again as in the frictionless case. In fact, Eqs. (50) and (51) are found to reduce (as they should) to Eqs. (21) and (22) from the frictionless case when all the c_k's are equal to cero.

5. Limitations of the model

The general equation for the normal force over the rolling sphere must be derived for the case with friction (and thus implicitly for the frictionless case) in order to obtain its limitations: the sphere is no longer restricted to move under the holonomic constraint if the magnitude of the normal force is negative at any moment, for it would stop being in contact with the surface and thus its motion would be unconstrained. To accomplish this we proceed to use the method of *Lagrange's Undetermined Multipliers* with the surfaces' holonomic constraint, which is useful when "you wish to determine forces of constraint using the Lagrangian approach" [12].

The following holonomic constraint for the motion of the sphere was introduced for the frictionless case since it is just the surface Eq. (3):

$$f(z,\rho) = z - a(\rho - h)^n = 0. \tag{53}$$

In order to use Lagrange's multipliers to obtain the normal force on the sphere as a function of time, we let each one of Lagrange's equations to be [5]:

$$\frac{d}{dt}\left(\frac{\partial \mathcal{L}}{\partial \dot{q}_i}\right) - \frac{\partial \mathcal{L}}{\partial q_i} - Q_i = \lambda \frac{\partial f}{\partial q_i}, \tag{54}$$

where λ is called the Lagrange Multiplier and f is the previous holonomic constraint. This equation must be used for each coordinate without substituting the holonomic constraint in the left side of Eq. 54, for we must deal with more equations than degrees of freedom in order to use the Lagrange Multipliers and get to know the constraint forces [13].

The generalized constraint force corresponding to the ith generalized coordinate is given by [5]:

$$F_i = \lambda \frac{\partial f}{\partial q_i}. \tag{55}$$

This generalized force "is a force if the corresponding generalized coordinate is a spatial coordinate and a torque if the corresponding generalized coordinate is an angular coordinate" [14]. For each of our three cylindrical coordinates we get:

$$F_\rho = \lambda \frac{\partial f}{\partial \rho} = -\lambda a n(\rho - h)^{n-1},$$

$$F_z = \lambda \frac{\partial f}{\partial z} = \lambda,$$

$$F_\phi = \lambda \frac{\partial f}{\partial \phi} = 0,$$

As we can see, there is no generalized force (torque) on the ϕ coordinate due to the azimuthal symmetry of the system, and therefore, the normal force will be the norm of the normal force vector (56):

$$\vec{N}(t) = \lambda \frac{\partial f}{\partial \rho}\hat{\rho} + \lambda \frac{\partial f}{\partial z}\hat{z} \tag{56}$$

$$|\vec{N}(t)| = \left(\sum_{i=1}^{3} F_i^2\right)^{1/2} = \sqrt{\left(\lambda \frac{\partial f}{\partial \rho}\right)^2 + \left(\lambda \frac{\partial f}{\partial z}\right)^2}$$

$$= \lambda(1 + a^2 n^2 (\rho - h)^{2(n-1)})^{1/2}. \tag{57}$$

Now we want to eliminate λ from (57) to obtain $|\vec{N}(t)|$ as a function of the coordinates whose behavior we already know from Eqs. (50) and (51). By doing a similar procedure as in Sec. 4.1 to obtain Q_ρ for the ρ-coordinate but now without substituting the holonomic constraint in the equation for the squared speed (using Eq. (4) as shown), we get:

$$Q_\rho = \vec{F} \cdot \frac{\partial \vec{v}}{\partial \dot{\rho}} = -\psi(|\vec{v}|)\frac{\partial |\vec{v}|}{\partial \dot{\rho}} = -\psi(|\vec{v}|)\frac{\partial}{\partial \dot{\rho}}$$

$$\times (\dot{\rho}^2 + \rho^2 \dot{\phi}^2 + \dot{z}^2)^{1/2} = -\left(\sum_{k=1}^{N} c_k |\vec{v}|^{k-1}\right)\dot{\rho}. \tag{58}$$

Now, by substituting Q_ρ and F_ρ into Eq. 54 for the ρ-coordinate, remembering not to substitute the holonomic constraint into the Lagrangian at its left-hand side, and calculating the corresponding partial derivatives, we obtain Eq. 59:

$$m(1+k)(\ddot{\rho} - \dot{\phi}^2 \rho) + \left(\sum_{k=1}^{N} c_k |\vec{v}|^{k-1}\right)\dot{\rho}$$

$$= -\lambda a n(\rho - h)^{n-1}. \tag{59}$$

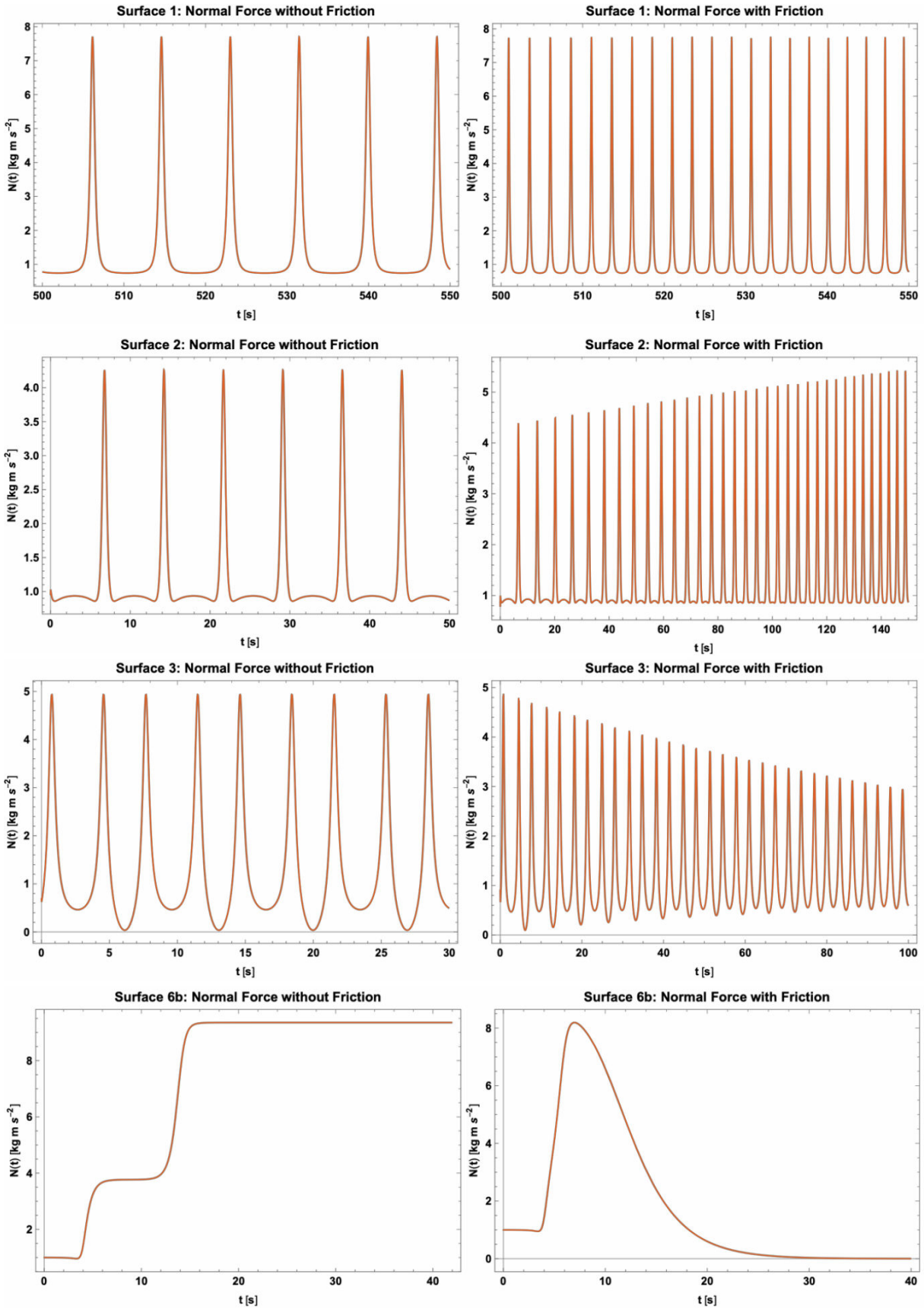

FIGURE 30. Plot of the normal force that the surfaces exert over the rolling sphere in special cases 1, 2, 3, and 7, both with and without friction as described in "Friction Parameters".

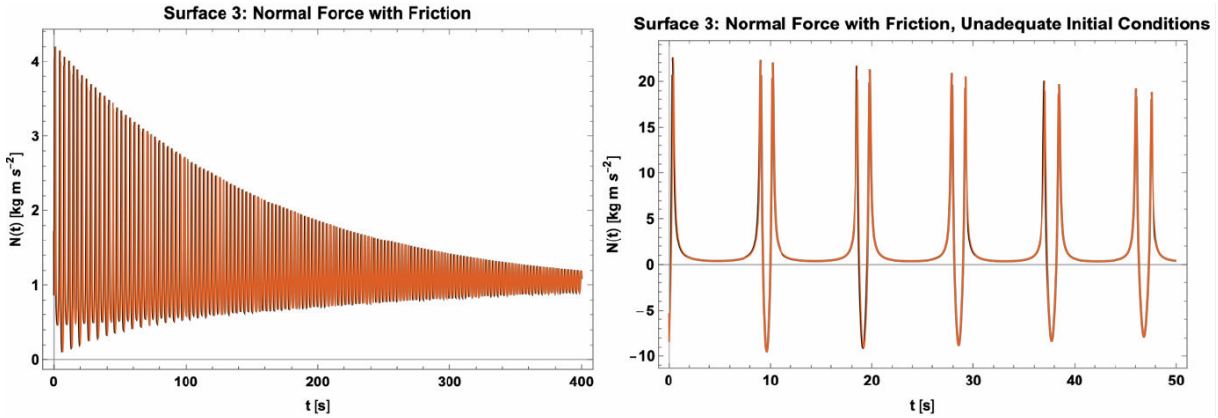

FIGURE 31. Plot of the normal force that the Surface 3 exerts over the rolling sphere from special case 3 and a modified version of it with $\dot{\phi}(0) = 3$, both with friction as described in "Friction Parameters".

A thorough procedure to obtain this last equation can be found in the section "Appendix 2: Obtaining Eq. (59)". Alternatively, by isolating the Lagrange Multiplier λ we get:

$$\lambda = -\frac{1}{an(\rho-h)^{n-1}}\left(m(1+k)(\ddot{\rho}-\dot{\phi}^2\rho) + \left(\sum_{k=1}^{N} c_k|\vec{v}|^{k-1}\right)\dot{\rho}\right). \tag{60}$$

Therefore, we find by substituting (60) into (57) that the normal force's modulus as a function of time will be

$$|\vec{N}(t)| = -\frac{1}{an(\rho-h)^{n-1}}\left(m(1+k)(\ddot{\rho}-\dot{\phi}^2\rho) + \left(\sum_{k=1}^{N} c_k|\vec{v}|^{k-1}\right)\dot{\rho}\right) \times (1+a^2n^2(\rho-h)^{2(n-1)})^{1/2}. \tag{61}$$

Let us recall that in order for the model to be valid at all times, the condition

$$|\vec{N}(t)| \geq 0 \tag{62}$$

must always be met, meaning that if $|\vec{N}(t)|$ is at some time t_0 a negative function of t, then the equations of motion (50) and (51) will stop describing the real motion of the system because it will dissatisfy the holonomic constraint (53).

Examples of such function $|\vec{N}(t)|$ for some of the special cases used to illustrate the predictions from Secs. 2 and 4 are shown in Figs. 30 and 31 (note that $|\vec{N}(t)|$ is never negative in these cases).

We can see from the plots of Fig. 30 that the magnitude of the normal force can either decrease, increase, or stay the same throughout the motion of the sphere when it is in the presence of friction forces; while in the frictionless cases, the normal force describes a periodic behavior when stable orbits exist.

An interesting prediction that further exposes the differences between the friction and frictionless cases is that special case 7 with friction on Surface 6b is found to describe an asymptotic behavior to cero for the normal force, evidently as a consequence that the speed on the *azimuthal* coordinate also tends to cero, while in the frictionless case the normal force is found to have an asymptotic behavior to a constant positive value as the sphere keeps describing falling orbits around the z-axis.

Moreover, we can recall that the motion described in special case 3 tends to stop in a potential valley on Surface 3 as shown in Figs. 22 and 24, meaning that the normal force felt by the sphere should tend to $|\vec{N}(t)| = mg$ as time tends to infinity, exactly as shown in Fig. 31 (recall that for special case 3 we have $m = 1$ and $g = 1$).

It is also important to show the plot of the normal force's modulus function (61) when the necessary conditions needed to satisfy condition (62) are not met, as illustrated in Fig. 31 and created by using the initial condition $\dot{\phi}(0) = 3$ that makes the sphere have enough speed to stop being in contact with the surface, thus forcing it to dissatisfy the holonomic constraint (53). All of the examples previously provided in this paper follow at all times the condition (62), which is easily unmet by letting the initial conditions describe a sufficiently fast motion that turns $|\vec{N}(t)|$ into a negative function of t and thus, make the sphere and surface be related no more by the holonomic constraint.

6. Final remarks

The limitations and conditions of the models derived for the rolling sphere must be strictly considered in order to achieve the desired and previously described motion. These limitations offer a path of possible future research when considering distinct types of friction with diverse functional dependence on speed as well as the generalization to a wider space of surfaces that may not necessarily be azimuthally symmetric or single-termed functions of the radial coordinate.

Further modeling may involve more complex friction forces, since the one proposed in this research is strictly inaccurate as it does not consider the chaotic interaction between the rolling motion of the sphere and the air that surrounds it. Likewise, the interaction of the sphere with the surface itself remains unconsidered as neither the sphere nor the surface are in reality perfectly rigid bodies and may not necessarily follow at all times the rolling-without-slipping condition. In addition, diverse types of gravitational fields could be as well considered part of the system and may lead to further analogies with other force fields as considered here with Newtonian Gravitation and classically depicted elliptical orbits.

Appendix

A. Code in mathematica

Figure 32 shows the code used for the model with friction in *Wolfram Mathematica*.

B. Obtaining Eq. (59)

Here, the procedure to obtain Eq. (59) is shown. This equation comes from the substitution of a new Lagrangian (let us call it $\mathcal{L}'$) into the modified Euler-Lagrange equation (54) for the ρ-coordinate (Eq. B.1)

$$\frac{d}{dt}\left(\frac{\partial \mathcal{L}}{\partial \dot{\rho}}\right) - \frac{\partial \mathcal{L}}{\partial \rho} - Q_\rho = \lambda \frac{\partial f}{\partial \rho} \tag{B.1}$$

when the holonomic constraint (3) is not used and after the corresponding partial derivatives from the resulting equation are calculated.

The *Lagrangian* without substituting the constraint (as now required by the method of *Lagrange's Undetermined Multipliers*) is:

$$\mathcal{L}' = \frac{1}{2}m(1+k)|\vec{v}|^2 - V,$$

$$\mathcal{L}'(\rho, \dot{\rho}, \dot{\phi}, z, \dot{z}) = \frac{1}{2}m(1+k)(\dot{\rho}^2 + \rho^2\dot{\phi}^2 + \dot{z}^2) - mgz.$$

Note that the only difference with the Lagrangian 2.08 from section 2.1 was not substituting the holonomic constraint into $|\vec{v}|^2$ and V. Afterwards, all we have to do is to substitute this last *Lagrangian* $\mathcal{L}'$ into the modified *Euler-Lagrange* equation B.1 when $q_i = q_1 = \rho$ and calculate the corresponding partial derivatives:

```
In[ ]:= ClearAll[a, h, n, k, m, g, p0, p0dot, f0, f0dot, r, c1, c2, c3, c4]
        a = 1;
        h = 0;
        n = 1;
        k = 0.4;
        m = 1;
        g = 1;
        p0 = 1;
        p0dot = 1;
        f0 = 0;
        f0dot = 1;
        r = 0;
        c1 = 0.00; c2 = 0.00; c3 = 0.00; c4 = 0.00;
        v[t_] := ((1 + a^2 n^2 (p[t] - h)^(2 (n-1))) (p'[t])^2 + (p[t])^2 (f'[t])^2)^(1/2);
        z[t_] := a (p[t] - h)^n /. s;
        o[t_] := -1/(a n (p[t] - h)^(n-1)) (m (1 + k) (p''[t] - (f'[t])^2 (p[t])) + (Sum_{i=1}^{r} ((Symbol["c" <> ToString[i]]) (v[t])^(i-1))) (p'[t])) (1 + a^2 n^2 (p[t] - h)^(2 (n-1)))^(1/2) /. s
        s =
         NDSolve[
          {m (1 + k) ((1 + a^2 n^2 (p[t] - h)^(2 (n-1))) (p''[t]) + a^2 n^2 (n - 1) (p[t] - h)^(2 n-3) (p'[t])^2 - (p[t]) (f'[t])^2 + a n g (p[t] - h)^(n-1)/(1 + k)) +
            (Sum_{i=1}^{r} ((Symbol["c" <> ToString[i]]) (v[t])^(i-1))) (1 + a^2 n^2 (p[t] - h)^(2 (n-1))) (p'[t]) == 0,
          m (1 + k) ((p[t])^2 (f''[t]) + 2 (p[t]) (p'[t]) (f'[t])) + (Sum_{i=1}^{r} ((Symbol["c" <> ToString[i]]) (v[t])^(i-1))) (p[t])^2 (f'[t]) == 0,
          p[0] == p0, p'[0] == p0dot, f[0] == f0, f'[0] == f0dot}, {p, f}, {t, 10000}]

Out[ ]= {{p → InterpolatingFunction[ Domain: {{0., 1.00×10^4}} Output: scalar  Data not in notebook; Store now »
         , f → InterpolatingFunction[ Domain: {{0., 1.00×10^4}} Output: scalar  Data not in notebook; Store now »
         ]}}
```

FIGURE 32. Code used in *Wolfram Mathematica* to obtain the solutions to the equations of motion required to produce the graphs and plots for special case 1, a similar procedure (with different parameters) was used to obtain the solutions to the other cases. "$o[t\_]$" represents the Normal Force Function $N(t)$, likewise "p" and "f" represent the coordinates ρ and ϕ, respectively.

$$\frac{\partial \mathcal{L}'}{\partial \rho} = m(1+k)\dot{\phi}^2\rho$$
$$\frac{\partial \mathcal{L}'}{\partial \dot{\rho}} = m(1+k)\dot{\rho}$$
$$\frac{d}{dt}\left(\frac{\partial \mathcal{L}'}{\partial \dot{\rho}}\right) = m(1+k)\ddot{\rho}$$

Now, by substituting these equations into (54) we get:

$$m(1+k)\ddot{\rho} - m(1+k)\dot{\phi}^2\rho - Q_\rho = \lambda\frac{\partial f}{\partial \rho},$$

or, simplifying:

$$m(1+k)(\ddot{\rho} - \dot{\phi}^2\rho) - Q_\rho = \lambda\frac{\partial f}{\partial \rho}.$$

Finally, by substituting the values found for Q_ρ in Eq. (58) and $\lambda(\partial f/\partial \rho)$ (in page 20) we get Eq. (59):

$$m(1+k)(\ddot{\rho} - \dot{\phi}^2\rho) + \left(\sum_{k=1}^{N} c_k|\vec{v}|^{k-1}\right)\dot{\rho} = -\lambda a n(\rho - h)^{n-1}.$$

1. J. Taylor, *Classical Mechanics* (University Science Books, Sausalito, CA, 2002), pp. 44, 238, 301.
2. W. Greiner, *Classical Mechanics*, 2nd ed. (Springer-Verlag Berlin Heidelberg, Frankfurt am Main, 2010), p. 275.
3. G. Arfken and H. Weber, *Mathematical Methods for Physicists*, 6th ed. (Elsevier Academic Press, 2005), p. 116.
4. MIT, Review B: Coordinate Systems, 2005, p. 6. Retrieved from http://web.mit.edu/8.01t/www/materials/modules/ReviewB.pdf
5. S. Thornton and J. Marion, *Classical Dynamics of Particles and Systems*, 5th ed. (Thomson Learning, Belmont, 2004), pp. 249, 250, 288.
6. V. Rochín and R. Paredes, *Las Leyes de Kepler y la Ley de Gravitación Universal.* (Instituto de Física, UNAM, 2014), p. 8. Retrieved from http://www.fisica.unam.mx/personales/romero/FC2014/Kepler-RP-VRR.pdf
7. P. Dourmashkin *et al.*, *Physics I: Classical Mechanics*. Module 28: The Kepler Problem: Planetary Mechanics, MIT OCW, (1999), p. 6. Retrieved from http://web.mit.edu/8.01t/www/materials/modules/guide17.pdf
8. P. Dourmashkin *et al. Physics I: Classical Mechanics*. Module 28: The Kepler Problem: Planetary Mechanics, MIT OCW, (1999), pp. 7, 8, 22. Retrieved from http://web.mit.edu/8.01t/www/materials/modules/guide17Appendix.pdf
9. J. Stewart, *Multivariable Calculus*, 7th ed. (Cengage Learning, Belmont, CA, 2012), p. 705.
10. R. Serway and J. Jewett, *Physics for Scientists and Engineers with Modern Physics*, 9th ed. (Pacific Grove, Boston, MA, 2014), p. 318.
11. H. Goldstein, C. P. Poole, and J. L. Safko, *Classical Mechanics*. (Pearson Education, Delhi, 2006), pp. 19, 23.
12. P. Saeta, *Lagrange Multipliers*. (Harvey Mudd College, 2013), p. 5. Retrieved from http://www.physics.hmc.edu/∼saeta/courses/p111/uploads/Y2013/lec130925-LagrangeMultipliers.pdf
13. J. T. Wheeler, *Mechanics, Constraints*. (Utah State University, 2012), p. 109. Retrieved from: http://www.physics.usu.edu/Wheeler/ClassicalMechanics/MechanicsBookFall2014.pdf
14. Dzierba, *Forces of Constraint & Lagrange Multipliers*, (2006), p. 5. Retrieved from http://www.dzre.com/alex/P442/lectures/lec_30.pdf